(Im)mobilization of iron, manganese, and arsenic during managed aquifer recharge in Bangladesh

Push-pull tests under oxidative and reductive conditions

Rafiq, Muhammad Risalat; Kruisdijk, Emiel; Ahmed, Kazi Matin; Rietveld, Louis C.; van Breukelen, Boris M.

DOI
10.1016/j.watres.2025.124878

Publication date
2025

Document Version
Final published version

Published in
Water Research

Citation (APA)
Rafiq, M. R., Kruisdijk, E., Ahmed, K. M., Rietveld, L. C., & van Breukelen, B. M. (2025). (Im)mobilization of iron, manganese, and arsenic during managed aquifer recharge in Bangladesh: Push-pull tests under oxidative and reductive conditions. *Water Research*, *289*, Article 124878. https://doi.org/10.1016/j.watres.2025.124878

Water Research 289 (2026) 124878

Contents lists available at ScienceDirect

Water Research

journal homepage: www.elsevier.com/locate/watres

(Im)mobilization of iron, manganese, and arsenic during managed aquifer recharge in Bangladesh: Push-pull tests under oxidative and reductive conditions

Muhammad Risalat Rafiq [a,b,*], Emiel Kruisdijk [a], Kazi Matin Ahmed [c], Louis C. Rietveld [a], Boris M. van Breukelen [a]

[a] Delft University of Technology, Faculty of Civil Engineering and Geosciences, Department of Water Management, Stevinweg 1, 2628 CN Delft, the Netherlands
[b] University of Barishal, Faculty of Science and Engineering, Department of Geology and Mining, Barishal 8254, Bangladesh
[c] University of Dhaka, Faculty of Earth and Environmental Sciences, Department of Geology, Dhaka 1000, Bangladesh

HIGHLIGHTS

- Fourteen (14) Push-Pull Tests (PPTs) were conducted under oxidative and reductive conditions at four (4) managed aquifer recharge (MAR) sites of SW Bangladesh.
- PPTs appeared crucial in understanding the main hydrogeochemical processes when oxic fresh water was temporarily stored and reactive organic matter was introduced into anoxic brackish aquifers.
- The consumption of dissolved oxygen (DO) was rapid during oxidative PPTs, and its rate appeared much higher than observed in other aquifers, which can be explained by heterogeneous Fe oxidation at all sites.
- Reductive PPTs demonstrated the risk for Fe, Mn, and As mobilization when reactive organic matter induces iron-oxide reduction.
- Limiting the introduction of reactive organic matter during infiltration and keeping conditions oxic during storage prevents mobilization and promotes immobilization of Fe, Mn, and As on iron-oxides at MAR systems of Bangladesh.

GRAPHICAL ABSTRACT

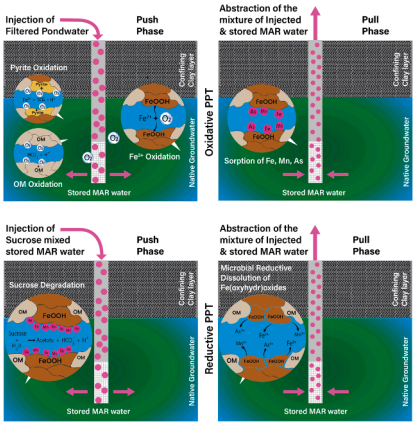

* Corresponding author at: Delft University of Technology, Faculty of Civil Engineering and Geosciences, Department of Water Management, Stevinweg 1, 2628 CN Delft, the Netherlands.
E-mail address: m.r.rafiq-1@tudelft.nl (M.R. Rafiq).

https://doi.org/10.1016/j.watres.2025.124878
Received 31 July 2025; Received in revised form 28 October 2025; Accepted 30 October 2025
Available online 31 October 2025

ARTICLE INFO

Keywords:
Aquifer storage and recovery
Groundwater quality
Redox processes
Geogenic metals
Arsenic mobilization

ABSTRACT

Managed Aquifer Recharge (MAR) systems have supplied drinking water to rural communities in southwestern Bangladesh since 2009. Although MAR enhances water availability, there are concerns about the potential mobilization of iron (Fe), manganese (Mn), and arsenic (As) during storage. Fourteen push-pull tests (PPTs) were performed under oxidative and reductive conditions at four MAR sites. These tests involved injecting filtered and O_2-saturated pond water for oxidative conditions, and sucrose-amended anoxic stored MAR water for reductive conditions, via a well in the stored MAR water. During oxidative PPTs, repeated aeration, injection, and abstraction cycles resulted in rapid consumption of dissolved oxygen (DO) with first-order rate constants of ~52 to 72 day^{-1} across all sites. DO was mainly consumed by adsorbed and dissolved Fe, with no apparent signs of pyrite and organic matter (OM) oxidation. The consistently high rate constant across the cycles suggests that heterogeneous Fe oxidation dominates. DO oxidizes Fe(II) to form Fe-(oxyhydr)oxides, resulting in the temporary removal of dissolved Fe (~98 %), Mn (~70–80 %), and As (60–70 %) at sites GMF11 and JJS91 due to sorption onto newly formed Fe-(oxyhydr)oxides. At sites MGS and MF05, increased As concentrations were noted due to the desorption of As from the Fe-(oxyhydr)oxides surface during abstraction. During reductive PPTs, the sucrose degraded over time, resulting in increased bicarbonate (HCO_3) and acetate concentrations and decreased pH and (sucrose-derived) DOC in abstracted water. These conditions led to the reductive dissolution of Fe-(oxyhydr) oxides, mobilizing Fe, Mn, and As, resulting in concentration peaks up to 70 mg/L Fe, 3.5 mg/L Mn, and 120 μg/L As. At MGS and MF05, similar trends for Fe and Mn were observed, while As levels did not increase. Peak concentrations were observed after about one day at JJS91, and two days at the other sites. Regular infiltration of O_2-saturated water may limit mobilization of Fe, Mn, and As, while the occurrence of reduced conditions should be prevented, as they could result in mobilization of these geogenic metals and endanger the provision of safe drinking water.

1. Introduction

The United Nations Sustainable Development Goal (SDG) 6 aims to increase access to clean, safe water and proper sanitation (Ho et al., 2020; Küfeoğlu, 2022). This is particularly important in the Khulna, the Satkhira, and the Bagerhat districts in southwestern (SW) Bangladesh, where drinking water sources are scarce and often unsafe (Naus et al., 2021). In these regions, communities face a shortage of fresh drinking water due to saline surface and groundwater (Naus et al., 2019). Regrettably, water availability is further deteriorated by contamination of fresh pond water with pathogens and bacteria (Alam et al., 2006; Bhuiyan et al., 2011), reduced infiltration due to urbanization (Abedin et al., 2019; Khan et al., 2014), rise in seawater levels due to climate change (Sarker et al., 2021, 2018), and contamination of shallow groundwater with arsenic (Ayers et al., 2016; Harvey et al., 2002; Naus et al., 2021). Recently, steps have been taken towards achieving SDG 6 to enhance freshwater availability by implementing Managed Aquifer Recharge (MAR) systems in this region (Sultana et al., 2015).

MAR is a freshwater management system that stores surplus fresh water in a shallow aquifer during the wet season, which can then be abstracted during the dry season to meet the community's water demands (Missimer and Maliva, 2010; Pyne, 2017). From 2009 to 2014, 99 MAR systems were constructed to provide fresh and safe drinking water in the Khulna, the Satkhira, and the Bagerhat districts of SW Bangladesh (Naus et al., 2021). MAR systems can operate through either injection or infiltration methods; however, in SW Bangladesh, they are predominantly infiltration-based. At these MAR systems, fresh water is collected from surface water (pond) and rooftops, treated for turbidity in a sand filtration tank and subsequently infiltrated into brackish to saline confined aquifers (background EC ranging 1.0 to 19 mS/cm) using several infiltration wells (Barker et al., 2016; Hasan et al., 2018). The stored water is abstracted year-round using a hand-operated tube well for drinking water purposes, without further treatment, only when its quality, particularly salinity and arsenic levels, meets safe and acceptable standards, as monitored monthly (Hasan et al., 2018).

MAR systems offer a sustainable solution for ensuring a consistent potable water supply (Naus et al., 2021), and they can naturally purify water through filtration, sorption, and biodegradation processes due to sediment-water interactions (Antoniou et al., 2012; Kruisdijk et al., 2022). However, the potential mobilization of arsenic (As) from the arsenic-rich aquifers in Bangladesh should be studied carefully to ensure that safe drinking water is provided. Pyrite and arsenopyrite are primary host minerals for As in the Bengal basin sediments (Chakraborty et al., 2015; Lowers et al., 2007; Zheng et al., 2004). Introducing oxygenated water into the aquifer due to excessive groundwater pumping promotes the oxidative dissolution of arsenic-bearing sulfide minerals, leading to elevated As concentrations in the shallow groundwater of the Bengal basin (Das et al., 1995). However, other studies indicate that released As can be adsorbed onto Fe-(oxyhydr)oxides during pyrite oxidation, thereby limiting groundwater As concentrations (McArthur et al., 2001; Savage et al., 2000). Moreover, the Holocene sediments of the Bengal basin are generally rich in organic matter (Anawar et al., 2010), and microbial reductive dissolution of Fe-(oxyhydr)oxides, is the predominant and accepted hypothesis for As mobilization in shallow groundwater for this region (Biswas et al., 2014; Chapelle, 2000; McArthur et al., 2004; Nickson et al., 2000). Therefore, pyrite minerals still play a critical role in releasing As and facilitating its repartitioning onto Fe-(oxyhydr)oxides, while microbial reductive dissolution of Fe-(oxyhydr)oxides mobilizes As into the groundwater of the Bengal Basin.

At the MAR systems in SW Bangladesh, fresh infiltration water introduces both dissolved oxygen (DO; ~8.0 mg/L) and dissolved organic matter (OM; ~9.5 mg/L as dissolved organic carbon) into anoxic brackish aquifers. DO can oxidize dissolved Fe(II) in native groundwater to form Fe-(oxyhydr)oxides, which are well-known adsorbents for As and manganese (Mn) (Annaduzzaman et al., 2020; Rahman et al., 2014; van Halem et al., 2010). However, water quality can also deteriorate during storage as DO becomes fully consumed by reductants, such as organic matter (OM) and pyrite (Antoniou et al., 2013; Kruisdijk and van Breukelen, 2021; Zuurbier et al., 2016). OM oxidation can result in increased ammonia (NH_4) and phosphate (PO_4) concentrations, while, more importantly, pyrite oxidation often results in increased As concentrations in the recovered water. Furthermore, the infiltration of DO-rich water prevents reduced conditions, which could trigger the reductive dissolution of Fe-(oxyhydr)oxides, leading to the mobilization of Fe, Mn, and As in the recovered water (Antoniou et al., 2012; Fakhreddine et al., 2021; Neil et al., 2012). Prolonged storage periods without infiltration might, however, lead to these conditions, with consequently substantial deterioration of the recovered water. A recent study by Rafiq et al. (2022) observed that As desorption and siderite dissolution led to the mobilization of Fe, Mn, and As at these sites. Desorption occurred when the pond water with low As concentrations was infiltrated, and the native groundwater was displaced.

Research on As mobilization in shallow aquifers of Bangladesh has been extensive to ensure safe drinking water (Ahmed et al., 2004; Aziz et al., 2017; Bhattacharya et al., 2009; Hasan et al., 2007; Mladenov et al., 2010; Ravenscroft et al., 2005). While mobilization of As, including the impact of DO and dissolved organic carbon (DOC), has been studied in both natural aquifers and MAR systems around the world (Fakhreddine et al., 2020; Kruisdijk and van Breukelen, 2021), little is known about how these processes occur in anoxic and brackish to saline aquifers, particularly in Bangladesh. The conditions and processes in a MAR system differ significantly from those of fresh groundwater abstraction, notably in the introduction of DO and OM in anoxic and brackish to saline aquifers. Therefore, further study is needed under field conditions, explicitly addressing the potential for Fe, Mn, and As (im) mobilization under oxidative and reductive conditions in the MAR systems of Bangladesh.

Push-pull tests (PPTs) are a well-known method for obtaining quantitative information on in-situ biogeochemical processes (Kruisdijk et al., 2022; Kruisdijk and van Breukelen, 2021). During a typical PPT, a solution with known composition is injected into the subsurface via an existing groundwater well. Subsequently, the mixture of injected water and groundwater is extracted from the same well, and water quality changes during abstraction are analyzed (Istok, 2012; Istok et al., 1997). Numerous studies have demonstrated that PPTs can be applied to quantify rates of microbial processes, including aerobic respiration, denitrification (Kim et al., 2005; Kruisdijk et al., 2022; Schroth and Istok, 2006; Vandenbohede et al., 2008), and sulfate reduction (Schroth et al., 2001). The advantages of PPTs over lab and column experiments include the minimal disturbance of the analyzed sediments and the ability to investigate larger aquifer volumes under in-situ conditions (Istok, 2012; Vandenbohede et al., 2008). Moreover, PPTs resemble small aquifer storage and recovery (ASR) systems in which different reactants, such as DO and OM, are introduced to assess the reactivity of the aquifer (Kruisdijk and van Breukelen, 2021; Neidhardt et al., 2014; Radloff et al., 2017). To date, this method has rarely been applied at MAR sites, with the recent exception of the research by Kruisdijk et al. (2022); Kruisdijk and van Breukelen (2021), who used a reactive transport model to interpret and simulate the PPT data in an aquifer storage and recovery system in the Netherlands.

In this study, we applied PPTs at four MAR sites, with varying background As concentrations in native groundwater, to determine hydrogeochemical processes influencing the mobilization of Fe, Mn, and As under oxidative and reductive conditions in the MAR systems of SW Bangladesh. The study aimed to test three hypotheses. First, MAR in aquifers with As-containing pyrite may lead to the oxidative dissolution of pyrite. Second, DO consumption under oxidative conditions results in the oxidation of dissolved and (de)sorbed Fe(II) and consequent Fe, Mn, and As sorption onto the formed Fe-(oxyhydr)oxides. Third, longer periods without infiltration can result in reduced conditions and mobilization of Fe, Mn, and As due to the microbial reductive dissolution of Fe-(oxyhydr)oxides. We performed oxidative PPTs (injecting fully aerated filtered pond water) in successive cycles with the aim to assess the occurrence of pyrite oxidation. Furthermore, reductive PPTs (injecting sucrose-mixed anoxic MAR water) were performed with the aim to assess the occurrence of microbial reductive dissolution of Fe-(oxyhydr)

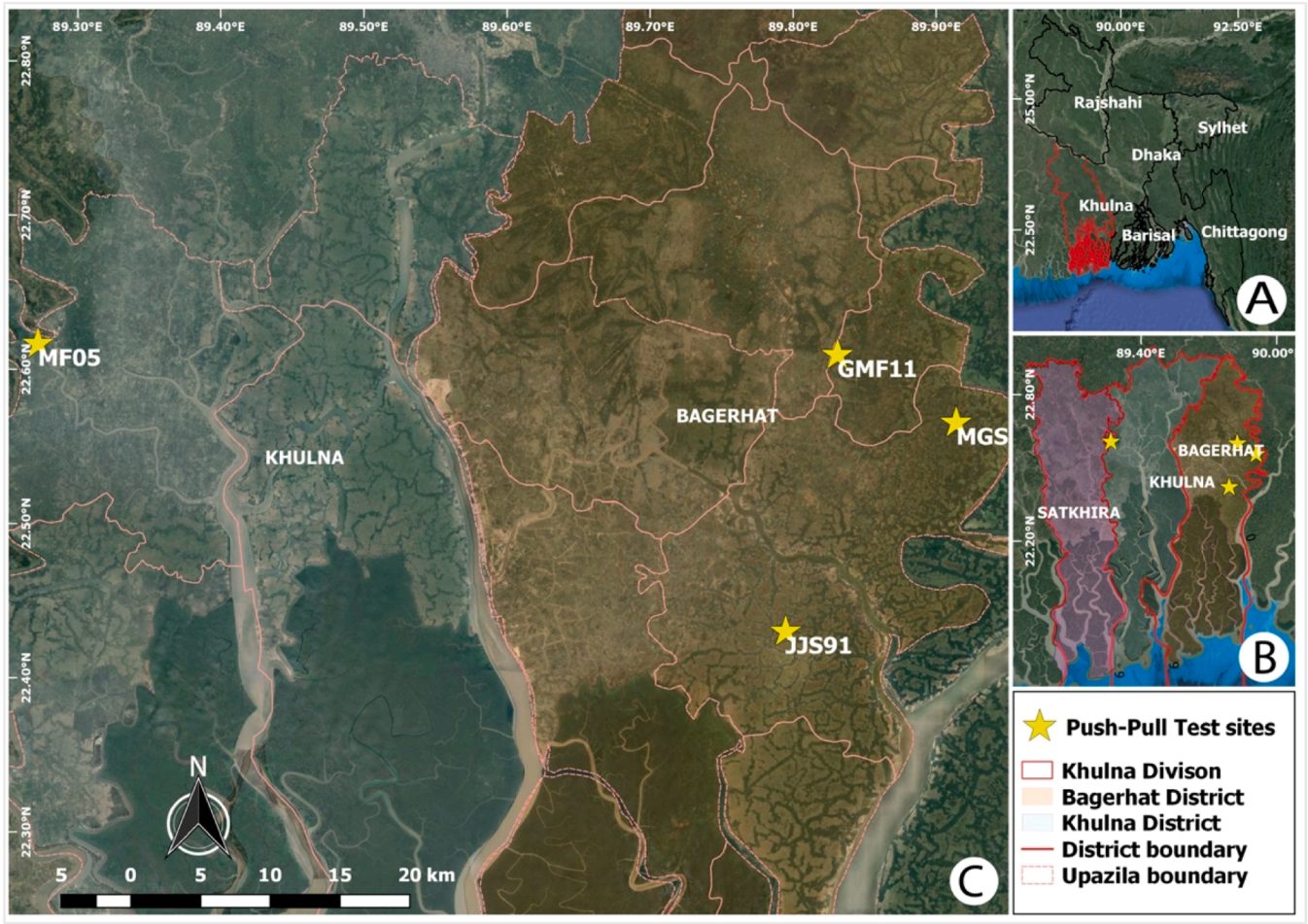

Fig. 1. Map prepared with QGIS (version 2.18.4) showing the locations of the four MAR sites (indicated with yellow stars) in the Bagerhat and the Khulna districts of SW Bangladesh (A-B). Among these MAR sites, JJS91 and MGS are in the Morrelganj upazila, GMF11 is in the Kachua upazila of Bagerhat, whereas MF05 is in the Paikgacha upazila of Khulna (C).

oxides.

2. Methods

2.1. Location of push-pull test sites

Oxidative and reductive push-pull tests (PPTs) were conducted at four MAR sites from October to November 2018: site GMF11 (22.622, 89.836), JJS91 (22.442, 89.804), and MGS (22.579, 89.919) are in the Bagerhat district, whereas MF05 (22.617, 89.278) is in the Khulna district of Bangladesh (Fig. 1). Arsenic (As) concentrations in the stored MAR water varied among these sites. At GMF11, concentrations (~ 72 μg/L) were observed above the Bangladesh drinking water standard of 50 μg/L, while JJS91 (~ 14 μg/L), MF05 (~ 8.5 μg/L), and MGS (~ 7.5 μg/L) were below this standard. The As concentrations reported herein were measured in the water sample collected during the PPTs. Before MAR operation, GMF11, JJS91, MGS, and MF05 all had higher As concentrations of 500 μg/L, 100 μg/L, 30 μg/L, and 50 μg/L, respectively. Table S4 in the supplementary document summarizes the operational and hydrochemical information of these MAR sites before this study. These sites were selected for their road accessibility, power availability, and logistical support compared to other MAR sites that showed comparable As levels.

We conducted PPTs at each site in the abstraction well, and in one monitoring well about 3.5 m from the abstraction well to replicate the results and evaluate aquifer heterogeneity. Table 1 shows the depth of the wells, additives used, and required volume for the push and pull phases during the PPTs at the selected MAR sites. The MAR system did not operate during the PPTs. At each site, we started with the oxidative (cyclic) PPT and followed with the reductive PPT.

2.2. MAR site layout

Freshwater from the local pond was the source of infiltration water at the four researched MAR sites. This water was treated with a sand filter for turbidity at approximately 2 m above ground level and then infiltrated under gravity into the anoxic and brackish sandy aquifers beneath clay layers of about 17 m thickness for MF05, 14 m for MGS, 12 m for GMF11, and 6 m for JJS91 (Fig. 2). Six large-diameter infiltration wells (diameter of ~0.25 m) were used for GMF11 and MF05, while JJS91 and MGS utilized four infiltration wells (diameter of ~0.30 m), all arranged in a circle with a radius of 1.8 m (Fig. 2). This array of four or six infiltration wells is primarily based on the required volume of water and the depth of the target aquifer. For the shallower aquifer systems, six wells were installed, whereas four wells were installed for the deeper systems for two main reasons: (a) the deeper aquifers possess relatively higher hydraulic conductivity than the shallower ones, allowing a higher volume of water to be injected through fewer wells; and (b) drilling wells at greater depth required higher expenses. The diameter of the infiltration wells varies in casing and screen dimensions at each site. For GMF11, each infiltration well has a depth of 24.4 m with a 12.2 m long screen; for JJS91, the depth is 22.3 m with a 15.2 m long screen; for MGS, the depth is 26 m with a 12.2 m long screen, and for MF05, the depth is 32 m with a 12.2 m long screen (see Fig. 2). At each site, an abstraction well (diameter: 0.05 m; screen length: 3.05 m) was centrally positioned in the system. This well was used to abstract stored freshwater using a hand-operated tube well for drinking water purposes, with depths ranging from 12.2 to 21.4 m for GMF11, 6.1 to 16.8 m for JJS91, 14 to 23 m for MGS, and 17 to 29 m for MF05 (Fig. 2). Each site maintains five monitoring wells with diameters and screen lengths like the abstraction wells at the respective sites. Additionally, one deep centre well (referred to as deep monitoring well) was installed at a depth of about 26 m for GMF11, 21 m for JJS91, 26 m for MGS, and 30.4 m for MF05. The other four observation wells (referred to as shallow monitoring wells 3–6) were positioned outside the circle of infiltration wells in a 3.66 m radius circle from the abstraction well, measured using a measuring tape, with screens at the same depth as the abstraction wells at four sites (see Fig. 2). The 1.8 m radius for the infiltration well array and the 3.66 m radius for the observation wells were established based on the preliminary conductivity survey and field constraints. However, no tracer test was conducted, and no regulatory guidelines or reference values from previous studies were available, as these MAR sites represented the first experiments in coastal Bangladesh. Closer well spacing was found to enhance aquifer freshening, while wider spacing produced isolated freshwater zones. Considering the low hydraulic gradient, limited land availability, and safety requirements for installing large-diameter (~0.3 m) wells, a compact circular layout was adopted.

2.3. Push-pull test (PPT)

Fig. 3 shows a schematic layout of a PPT where the water of known chemical composition is injected into the subsurface using an existing well, followed by the gradual abstraction of the mixture of injected water and groundwater from the same well (Istok et al., 1997; Kruisdijk and van Breukelen, 2021). In this study, we used filtered pond water (oxidative PPT) and stored MAR water (reductive PPT) as the injected water, which was stored in a 300 L tank before injection. The volume of injected water (push volume) during PPTs varied among the selected MAR sites, ranging from 210 to 300 L (Table 1). The water tank with a maximum capacity of 300 L was used at all sites due to its commercial availability, ease of transport, and comparability with previous studies of Kruisdijk and van Breukelen (2021). The push volume was calculated based on the volume of the PPT well, the volume of the gravel pack surrounding the well, and the number of water samples collected during each PPT. The combined volumes of the well and gravel pack were defined as the total dead volume, and the injected volume was calculated by multiplying the number of samples collected during PPT by the total dead volume. The injected water (push) volume was set to exceed this dead volume, ensuring that collected samples represented aquifer-resident water rather than water retained within the well or in the gravel pack. Conservative tracers, Br as NaBr, concentrations ranging from 0.01 to 0.08 mmol/L and Cl as NaCl, concentrations ranging from 0 to 1.4 mmol/L, as well as reactants, e.g., dissolved O_2 (DO), concentrations of ~8 mg/L and sucrose ($C_{12}H_{22}O_{11}$), concentrations of ~5 mmol/L), were added in injected water (Table 1). The sucrose dosage was considered based on previous studies in which reactive organic carbon was added to observe arsenic mobilization in the Bengal Delta aquifer (Neidhardt et al., 2014; Rawson et al., 2017). NaCl was only added if the difference in electrical conductivity (EC) between injected and stored MAR water was <100 μS/cm.

Table 1
Overview of PPTs conducted at MAR sites showing the depth of wells, types of condition, additives and volume of water used.

Site	Depth (m)	Mode of PPTs	Push water type	Additives	Dead volume (L)	Sample volume (L)	Push volume (L)	Pull Volume (L)
GMF11	22.0	Oxidative cyclic	Filtered pond water	O_2, NaBr	35	50	300	600
	22.0	Reductive	Anoxic SMW	Sucrose, NaCl and NaBr	-	50	300	300
JJS91	15.3	Oxidative cyclic	Filtered pond water	O_2, NaBr	25.5	40	240	480
	15.3	Reductive	Anoxic SMW	Sucrose, NaCl and NaBr		50	300	300
MGS	26.0	Oxidative cyclic	Filtered pond water	O_2, NaBr	22.5	35	210	420
MF05*	27.0	Oxidative cyclic	Filtered pond water	O_2, NaBr	43	50	300	600

* During PPTs, the abstraction well was used for all sites except MF05, where the (deep) monitoring well was used instead of the abstraction well.

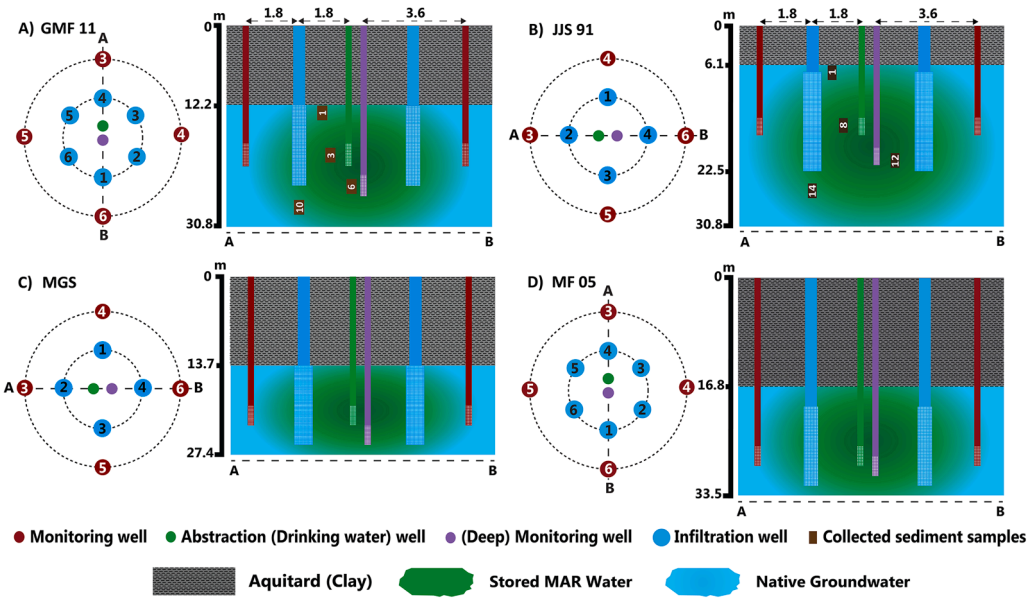

Fig. 2. Map (left) and cross-sectional (right) view of the wells of selected MAR sites (GMF11, JJS91, MGS, and MF05) where push-pull tests were conducted. Each cross-sectional (right) view shows the position and screen length of the infiltration, abstraction, and monitoring wells in each MAR system of the selected sites.

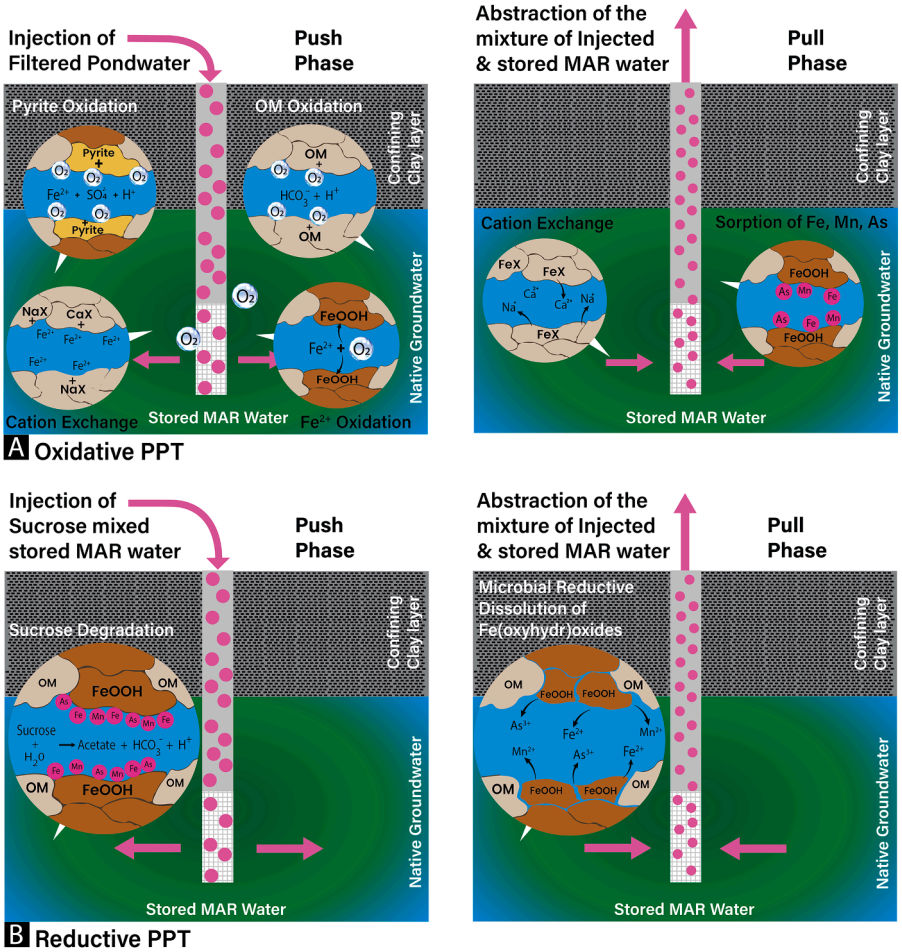

Fig. 3. Schematic layout of a push-pull test (PPT) under oxidative (A) and reductive conditions (B) to observe hydrogeochemical processes in aquifer. Filtered (fresh) pond water (A) and sucrose-mixed stored MAR water (B) are injected using existing abstraction or monitoring wells as part of the MAR systems (push phase, left panels) through the screen of the respective wells into the stored MAR water (green colour in all panels). The injected water (pink arrow in the left panel) is dispersed radially through the well screen into the stored MAR water. Subsequently, the mixture of the injected and the stored MAR water in the aquifer (pink arrow) is gradually abstracted from the same well (pull phase, right panel) and collected water samples are analysed for hydrochemical composition.

After thoroughly mixing the tracers and reactants using an aerator pump (~1.4 kW) in oxidative and a clean material (wooden stick) in reductive PPTs, the water was injected at a steady flow rate of approximately 9.5 L/min using a submersible pump (Eijkelkamp Gigant®). During the injection (push-phase), water samples were collected at three stages- beginning, middle, and end of injection following the standard water sampling procedures (Rafiq et al., 2022; Rahman et al., 2014), ensuring that the additives were thoroughly mixed and that the collected water samples represented the entire injection process. Moreover, onsite parameters were continuously recorded at 30-second intervals during the injection, indicating homogeneous mixing of the added chemicals (discussed in the Results section).

After a resting period of approximately 5 min, 12 water samples during oxidative PPTs and 6 during reductive PPTs were collected each time by abstracting 1.25 times the dead volume of the PPT well, ensuring that the sampled water volume came from the aquifer and not from the water inside the well (Kruisdijk and van Breukelen, 2021). Due to dispersion, the injected water was mixed with the existing stored MAR during the push phase. Therefore, even after abstracting the same volume of water that was injected, some of the injected water may remain in the aquifer. Therefore, twice the volume of injected water was abstracted in oxidative PPTs. In reductive PPTs, the abstracted water volume was equal to the injected volume (Table 1).

2.3.1. Oxidative (cyclic) PPTs

Filtered pond water was stored in a 300 L tank and was aerated with an aerator pump (~1.4 kW) until full DO saturation (~ 8 mg/L). Tracers and reactants were added during aeration when required (dosage mentioned before) and thoroughly mixed before injection (push phase of cycle 1). Injected water was collected during cycle 1 and indicated as IW 1. After the injection of cycle 1, four water samples were collected each time by abstracting 1.25 times the dead volume of the respective PPT well during the pull-phase. Approximately 20 mL of water was required during each sampling, and the rest was stored in the tank instead of being discarded. Around 80 % of the injected water was abstracted and stored in the same tank for aeration and injection in cycle 2. These aeration, injection, and abstraction phases were iterated twice (cycles 1 and 2), and in the final phase (cycle 3), twice the amount of injected volume was abstracted. During cycles 1 and 2, four water samples were collected in each cycle, while in cycle 3, 12 samples were collected with twice the volume being abstracted as injected. These successive cycles of aeration and injection allowed the introduction of sufficient DO in the aquifer to better observe the potential processes concerning the consumption of DO (Fig. 3A).

2.3.2. Reductive PPTs

During the reductive PPTs (Fig. 3B), stored MAR water from the selected PPT well was used as injected water instead of filtered pond water, and ~5 mmol/L sucrose ($C_{12}H_{22}O_{11}$, as reactive carbon) was added to the injected water to assess the reductive dissolution of Fe-(oxyhydr)oxides and the mobilization of As (Neidhardt et al., 2014; Rawson et al., 2017). Stored MAR water was abstracted using a submersible pump (Eijkelkamp Gigant®) and stored in a 300 L tank. The storage tank was kept closed to maintain anoxic conditions while the necessary procedures were performed quickly, likely resulting in slight increases in DO. The 300 L of sucrose-amended ($C_{12}H_{22}O_{11}$, ~5 mmol/L) water was injected under gravity into the PPT well (push--phase). The sucrose concentration of 5 mmol/L was adopted from the earlier and comparable studies of Rawson et al. (2017) and Neidhardt et al. (2014). With an incubation period of approximately 15 h, water samples were collected after abstracting 50 L of water, and 6 samples were collected during the pull phase. These samples were collected with a peristaltic pump (Solinst®410) twice a day, maintaining an interval of approximately 7 h until the total injected volume was abstracted. An incubation period of approximately 15 h was adopted to provide adequate time for the occurrence of microbially mediated reductive dissolution of Fe-(oxyhydr)oxides as reported in the comparable studies of Rawson et al. (2017) and Neidhardt et al. (2014). In addition, sampling at approximately 7-hour intervals also offered sufficient temporal resolution to monitor short-term fluctuations in Fe, Mn, and As mobilization.

2.4. Collection and analysis of aqueous and sediment samples

Water sampling and analysis: During the PPTs, water samples were collected from stored MAR water, injected water, and abstracted water following standard water sampling procedures (Rafiq et al., 2022; Rahman et al., 2014). Stored MAR water samples were collected from the abstraction and the monitoring well with a submersible pump (Eijkelkamp Gigant®) after purging triple the standing volume of the respective well, injected water samples were collected directly from a 300 L tank after adding additives, and abstracted water samples were collected with a peristaltic pump (Solinst®410) during the pull phase. Electrical conductivity (EC), temperature, pH/redox, and DO were measured directly on the field site and recorded using a PONSEL ODEON® multi-parameter meter throughout the experiment. The details of the PONSEL ODEON® multi-parameter probes for onsite measurement were described in Rafiq et al. (2022). During injection, these parameters (EC, temperature, pH/redox, and DO) were recorded continuously at 30-*sec* intervals by immersing individual PONSEL ODEON® multi-parameter probes in the 300 L tank. These parameters were also recorded every minute by immersing individual probes in a flow cell during the abstraction of water samples. Besides these parameters, alkalinity and turbidity were measured in the field using a digital titrator (HACH Method 10244) and a portable turbidity meter (HANNA HI 93703), respectively.

Collected water samples for laboratory analysis were stored in 15 mL plastic vials (SARSTEDT®) after filtration using a 0.45 μm filter. Water samples for major cations and trace elements (Na, K, Ca, Mg, Fe, Mn, As) were acidified 1/100 with 69 % HNO_3 (ACS, Merck®) and analyzed with inductivity coupled plasma mass spectrometry (ICP-MS; Analytik Jena model PlasmaQuant MS) after diluting the samples with acidified ultrapure water (1 % v/v). Water samples for anions (Cl, Br, F, SO_4, NO_3, NO_2, and acetate) were analyzed with a Metrohm® 818 ion chromatograph equipped with a Metrosep A supp 5–150/4.0 column. In addition, filtered water samples were collected for dissolved organic carbon (DOC) in 30 mL plastic vials (SARSTEDT®) and preserved with a 1 % concentrated HCl. These samples were analyzed using a Shimadzu® TOC analyzer (NPOC: non-purgeable organic carbon) after removing dissolved CO_2 by placing the samples in a vortex for 60 s (van Breukelen et al., 2003).

Sediment sampling and analysis: Ten sediment samples were collected from the aquifer at sites GMF11 and JJS91 with a modified split-spoon method (von Brömssen et al., 2008), where hand-flapper and hammer techniques were combined to perform the core drilling (Horneman et al., 2004). Detailed information on the depth and the method for sediment collection can be found in Rafiq et al. (2022). Grain size distribution and clay fraction were analyzed using Sympatec HELOS KR laser-diffraction (ranging from 0.15–2000 μm). The content of organic matter and calcium carbonate ($CaCO_3$) was measured using *LECO* thermogravimetric analysis (TGA; at 550 and 615–1000 °C). Bulk elemental concentrations were measured in XRF, and trace metals were measured in the ICP-MS by digestion utilizing Lithium Borate Fusion. The LECOC/S was used to determine the content of inorganic carbon and sulfur.

2.5. Calculation (and formulation) used in data interpretation

Sedimentary mineral content: The content of pyrite (FeS_2), pyrite bounded Fe, reactive Fe, and non-pyrite reactive Fe were estimated from the bulk elemental composition of S, Fe_2O_3, and Al_2O_3 according to the following equations (Griffioen et al., 2012; Kruisdijk and van Breukelen, 2021; Zuurbier et al., 2016):

$$FeS_2 = (0.5M_{FeS_2}/M_sS) \quad (1)$$

$$Fe_{py} = (0.5M_{Fe}/M_sS) \quad (2)$$

$$Fe_{TR} = \frac{2M_{Fe}}{M_{Fe_2O_3}}(Fe_2O_3 - 0.225Al_2O_3) \quad (3)$$

where M_{FeS_2}, M_{Fe} and M_s are the molecular weight of pyrite (g/mol), iron (g/mol), and sulfur (g/mol); and S is the content of sulfur in % d.w.

The following equation determined the content of Fe-oxides, which related to the calculated non-pyrite reactive Fe:

$$Fe_{reac} = (Fe_{TR} - Fe_{py}) \quad (4)$$

where the pyrite bounded Fe (Fe_{py}) and total reactive Fe (Fe_{TR}) were calculated using Eq. (2) and (3).

The cation exchange capacity (CEC) was estimated based on the clay fractions and organic matter percentage (Appelo and Postma, 2005). The formula used to calculate CEC is as follows:

$$CEC\left(\frac{meq}{kg}\right) = 7 \times (\%clay) + 35 \times (\%C) \quad (5)$$

where the fraction of clay (% d.w.) and content of organic carbon (% d.w.) are denoted as %clay and %C, respectively.

Conservative mixing lines of solutes during PPTs: Conservative concentrations (i.e., not influenced by processes besides advection and dispersion) of various solutes in abstracted water during PPTs were calculated using Eq. (7) based on mixing fractions of injected and stored MAR water, calculated using Cl concentrations, shown in Eq. (6), and the endmember concentrations of injected water and stored MAR water (Appelo and Postma, 2005). The conservative tracer Br (as NaBr) was added to the injected water to monitor mixing with native groundwater. The required amount of NaBr was determined by the molar ratio of Cl: Br. However, after processing and visualizing lab-analyzed data, it became apparent that Cl showed a clearer dispersion fit than Br due to the higher concentration difference. Therefore, Cl data was used instead of Br. The conservative mixing line can be compared to the concentrations of reactive constituents to highlight consumption (e.g., precipitation, sorption, degradation) or production (e.g., dissolution, desorption) of solutes.

$$f_{Cl} = \frac{m_{Cl,sample} - m_{Cl,IW}}{m_{Cl,SMW} - m_{Cl,IW}} \quad (6)$$

where the Cl-based fraction of injected water in abstracted water is denoted as f_{Cl}, and measured concentrations of Cl in injected water, stored MAR water, and abstracted water are denoted as $m_{Cl,IW}$, $m_{Cl,SMW}$, and $m_{Cl,sample}$, respectively.

$$m_{i,mix} = f_{Cl} \times m_{i,SMW} + (1 - f_{Cl}) \times m_{i,IW} \quad (7)$$

where the conservative mixing between injected water and stored MAR water is denoted by $m_{i,mix}$, the Cl-based fraction of injected water in abstracted water is denoted as f_{Cl}, the concentrations of a particular ion (i) for stored MAR water and injected water are denoted as $m_{i,SMW}$, and $m_{i,IW}$.

Reaction time and DO consumption rate: The plug-flow reactor model proposed by Schroth and Istok (2006) was used to determine the residence (i.e. reaction) time and the DO consumption rate, assuming a first-order reaction process. The residence time of each sample (j) collected during PPTs was calculated using the following formula of Schroth and Istok (2006):

$$t^j_{r,pf} = t^{*j} + \frac{\int_{t_{ext}=0}^{t^j_{ext}} Q_{ext}C_{tr}(t)dt}{M_{tr}} T_{inj} \quad (8)$$

where the residence time of each sample j is denoted as $t^j_{r,pf}$, the time elapsed since the end of injection as t^{*j}, the duration of injection phase as T_{inj}, the extraction rate during pull phase is denoted as Q_{ext}, the time since extraction as t_{ext}, and the total mass of tracer (electrical conductivity, EC) as M_{tr}.

Schroth and Istok (2006) assumed that the tracer concentrations (denoted as C_{tr} in Eq. (8)) range from 1 in the injected water concentration to 0 in native groundwater. However, in this study, the EC values were used as a conservative tracer, and EC values were higher in stored MAR water than in the injected water. Therefore, we normalized the tracer concentrations using the following Eq. (9):

$$C_{tr} = \frac{C_{sample} - C_{SMW}}{C_{IW} - C_{SMW}} \quad (9)$$

where the normalized tracer is denoted as C_{tr}, EC values of each sample during abstraction (pull-phase), injected and stored MAR water are represented as C_{sample}, C_{SMW}, and C_{IW}.

$$M_{tr} = C_{Inj(norm)} \times V_{Inj} \quad (10)$$

where the normalized tracer mass (total) is denoted as M_{tr}, the normalized EC of injected water is designated as $C_{Inj(norm)}$, and the total volume of injected water per cycle is denoted as V_{Inj}.

The DO consumption rate constants were estimated using the equation following from Schroth and Istok (2006).

$$\ln\left(\frac{C^*_r(t^*)}{C^*_{tr}(t^*)}\right) = -kt_{r,pf} \quad (11)$$

where the reactant (DO) and tracer values are denoted as C_r and C_{tr}, respectively.

The first-order rate constant was determined from the slope of a best-fitted line after plotting the data as $\ln\left(\frac{C^*_r(t^*)}{C^*_{tr}(t^*)}\right)$ vs. $t^j_{r,pf}$. The y-intercept of the fitted line in this linear regression was set to zero and the slope of this line was considered the DO consumption rate (Schroth and Istok, 2006).

Saturation index (SI) of minerals: The geochemical model PHREEQC interactive 3.0 for Windows (Parkhurst and Appelo, 1999) with the phreeqc.dat database was used to determine the saturation indices (SIs) of the following minerals: calcite ($CaCO_3$), dolomite ($CaMg(CO_3)_2$), and siderite ($FeCO_3$) in the analyzed water samples.

3. Results and discussion

3.1. Initial composition of injected and stored MAR water during PPTs

Table 2 presents the composition of the injected water and the stored MAR water during the oxidative (cyclic) PPTs at the four researched MAR sites and the composition of native groundwater (before MAR operation) when available. Generally, the stored MAR water appears relatively fresh (EC: 0.6–1.06 mS/cm) and anoxic (DO: ~ 0.0 mg/L) with a neutral pH (6.8–7.6). The Mn level in the stored MAR water was relatively higher (86–450 μg/L) compared to As at all sites, while Fe and As concentrations were highest at site GMF11 (Fe: 6.7 mg/L compared to 0.4–0.7 mg/L and As: 71 μg/L compared to ~8–14 μg/L). The saturation indices (SIs) for calcite and dolomite in stored MAR water at locations GMF11, JJS91, and MGS were below zero (SI < 0), indicating that the groundwater was undersaturated to these minerals during storage, whereas they were in equilibrium or slightly supersaturated in native groundwater. This suggests a potential for dissolution of calcite and dolomite during storage, which could consequently elevate the concentrations of Ca, Mg, and alkalinity. Similarly, the undersaturated siderite (SI < 0) in stored MAR water at JJS91 and MGS suggests its potential dissolution and contributes to increased levels of Fe and alkalinity. In contrast, the saturation index of siderite (SI ≥ 0) at GMF11 implies that siderite is likely to precipitate and subsequently reduce the concentrations of Fe and alkalinity. During the push-pull test (PPT)

Table 2
Composition of injected water (IW; i.e. filtered fresh pond water), stored MAR water (SMW), and native groundwater (NGW) during oxidative (cyclic) PPTs.

Parameters/concentrations of ions	GMF11			JJS91			MGS		MF05*	
	IW	SMW	NGW	IW	SMW	NGW	IW	SMW	IW	NGW
EC (mS/cm)	0.26	1.06	4.4	0.59	0.93	7.49	0.26	0.6	0.6	0.5
Temp (°C)	27.4	27.2	27.0	30.8	28.8	27.1	28	27.1	25.6	27.7
DO (mg/L)	8.4	0	0.0	7.9	0	0	8.5	0	8.8	0
pH (-)	8.3	7.04	7.0	8.2	6.8	6.7	8.4	7.6	8.4	7.8
Alkalinity (mg/L)	106	212	318	130	204	614	130	188	134	138
Cl (mg/L)	35.8	244	1367	115	232	1897	26.4	106	74.2	41.3
SO_4 (mg/L)	2.32	0	0.1	20.4	14.4	2.6	10.3	9.75	3.8	6.38
Na (mg/L)	16.2	140	742	69.3	136	1138	25.7	103	78.5	46.1
Ca (mg/L)	41	115	171	62.4	75	357	23.8	31.3	29.4	33.2
Mg (mg/L)	5.74	21.5	66.2	19.1	22.1	126	9.22	18.1	8.43	7.66
K (mg/L)	2.93	4.11	9.4	4.57	4.38	12.4	5.38	8.49	15.7	15
Fe (mg/L)	0.01	6.7	6.0	0.01	0.42	14.5	0.01	0.67	0.23	0.38
Mn (μg/L)	3.84	450	398	41.5	246	638	10.7	86.4	401	112
As (μg/L)	1.9	71.2	139	1.05	14.1	37.8	3.2	7.7	25.2	9.83
$SI_{Calcite}$	0.54	−0.07	0.1	0.7	−0.45	0.26	0.51	−0.12	0.53	0.03
$SI_{Dolomite}$	0.59	−0.51	0.1	1.3	−1.05	0.48	0.97	−0.12	0.88	−0.22
$SI_{Siderite}$	−0.81	0.89	0.9	−0.97	−0.51	1.03	−0.89	0.38	0.51	0.27

* An abstraction well was used for all sites except MF05, where the (deep) monitoring well was used instead of the abstraction well. Approximately 1.4 mmol/L of NaCl was added to the injection water and injected into NGW instead of SMW.

experiment at site MF05, the abstraction well was non-functional. Consequently, a (deep) monitoring well was used at this site, and filtered pond water was injected into the native groundwater instead of the stored MAR water.

The data presented in Table 2 indicate that the water used for the push-phase of the PPTs was fresh and completely saturated with O_2 at all four MAR sites, as evidenced by the lower EC values, major ion concentrations, and higher DO levels compared to stored MAR water, while pH was considerably higher due to CO_2 stripping during aeration. Fe (0.01–0.23 mg/L), Mn (~4–11 μg/L), and As (~1–25 μg/L) concentrations in the injected water were low at each site, except for site JJS91, where the Mn concentration was 41.5 μg/L, and for MF05, where the As concentrations was ~400 μg/L. The positive SIs values for calcite and dolomite (0.5–1.3) show that the injected water, likely due to CO_2 stripping, was supersaturated to these minerals and thus had the potential to precipitate. Conversely, the negative SIs values for siderite (−0.8 to −0.97) indicate undersaturation, meaning siderite might dissolve. Table 3 presents the composition of the stored MAR and injected water, where the injected water is the prior abstracted stored MAR water after the addition of sucrose and NaCl.

3.2. Hydrogeochemical processes during oxidative PPT at GMF11

We selected site GMF11 as a reference for comprehensive interpretation because (i) it represents the data and hydrogeochemical processes clearly, making it easier for the reader to understand (Fig. 4); and (ii) it effectively highlights the key processes, enabling a comprehensive comparison with the other three sites.

Figure S1 (in the supplement) displays the continuously measured onsite parameters of injected water, including EC, temperature, pH, and DO, during the three injection phases (cycles). During each cycle, it took approximately 30 min to inject aerated water at an average rate of 9.7 L/min. The sensed parameters remained nearly stable (EC and DO) except for temperature and pH. The temperature increased by 0.7 °C from cycle 1 to 3 due to increased air temperatures during the day. Similarly, the pH increased by 1.4 units compared to stored MAR water, due to CO_2 stripping that occurred during aeration (Appelo and Postma, 2005). The nearly stable sensed parameters in Figure S1 (supplement) and Table 4

Table 3
Composition of stored MAR water (SMW) and injected water (IW: sucrose and required additives added to SMW) during reductive PPTs.

Parameters/concentrations of ions	GMF11		JJS91		MGS		MF05	
	SMW	IW	SMW	IW	SMW	IW	SMW	IW
EC (mS/cm)	1.05	1.17	1.59	1.70	0.49	0.73	0.41	0.56
Temp (°C)	27.2	27.6	28.75	28.78	26.55	26.44	27.46	27.47
pH (-)	6.8	7.1	7.0	7.3	8.8	8.6	7.7	7.8
ORP (mV)	34.9	−111.7	−36.4	5.43	127.7	90.7	3.5	−0.98
DOC (mg/L)	7.88	755	7.3	758	6.8	713.4	10.2	778.5
Alkalinity (mg/L)	216	252	236	256	208	204	134	134
Cl (mg/L)	257	279	305	329	60.6	108	42	73
SO_4 (mg/L)	0.0	0.0	13.7	14.4	12.1	3.1	6.4	5.4
Na (mg/L)	153	192	242	279	62	111	46.2	83.2
Ca (mg/L)	117	115	87.6	88.4	38.6	42.8	32.6	33.9
Mg (mg/L)	22.2	21.4	27.9	28.2	21.4	23.9	8.2	8.3
K (mg/L)	5.1	5.3	5.0	5.0	10.6	11.3	15.2	16.2
Fe (mg/L)	1.7	2.3	0.2	0.2	0.03	0.02	0.04	0.04
Mn (ug/L)	545	539	272	287	36.9	48.7	112	99
As (ug/L)	72.9	86.8	15.4	16.6	15.2	15.2	27.3	16.0
$SI_{Calcite}$	−0.25	0.05	−0.15	0.11	1.18	0.97	−0.02	0.03
$SI_{Dolomite}$	−0.86	−0.26	−0.43	0.09	2.47	2.06	−0.29	−0.20
$SI_{Siderite}$	0.10	0.53	−0.67	−0.37	−0.04	−0.49	−0.74	−0.71

*The abstraction well was used at sites GMF11 and JJS91 and the monitoring well was used at sites MGS and MF05. Approximately 5 mmol/L of sucrose was added to SMW at each site. Additionally, at sites GMF11 and MGS, approximately 1.1 mmol/L of NaCl was added to SMW, while at sites JJS91 and MF05, 2 mmol/L and 1.4 mmol/L of NaCl were added, respectively.

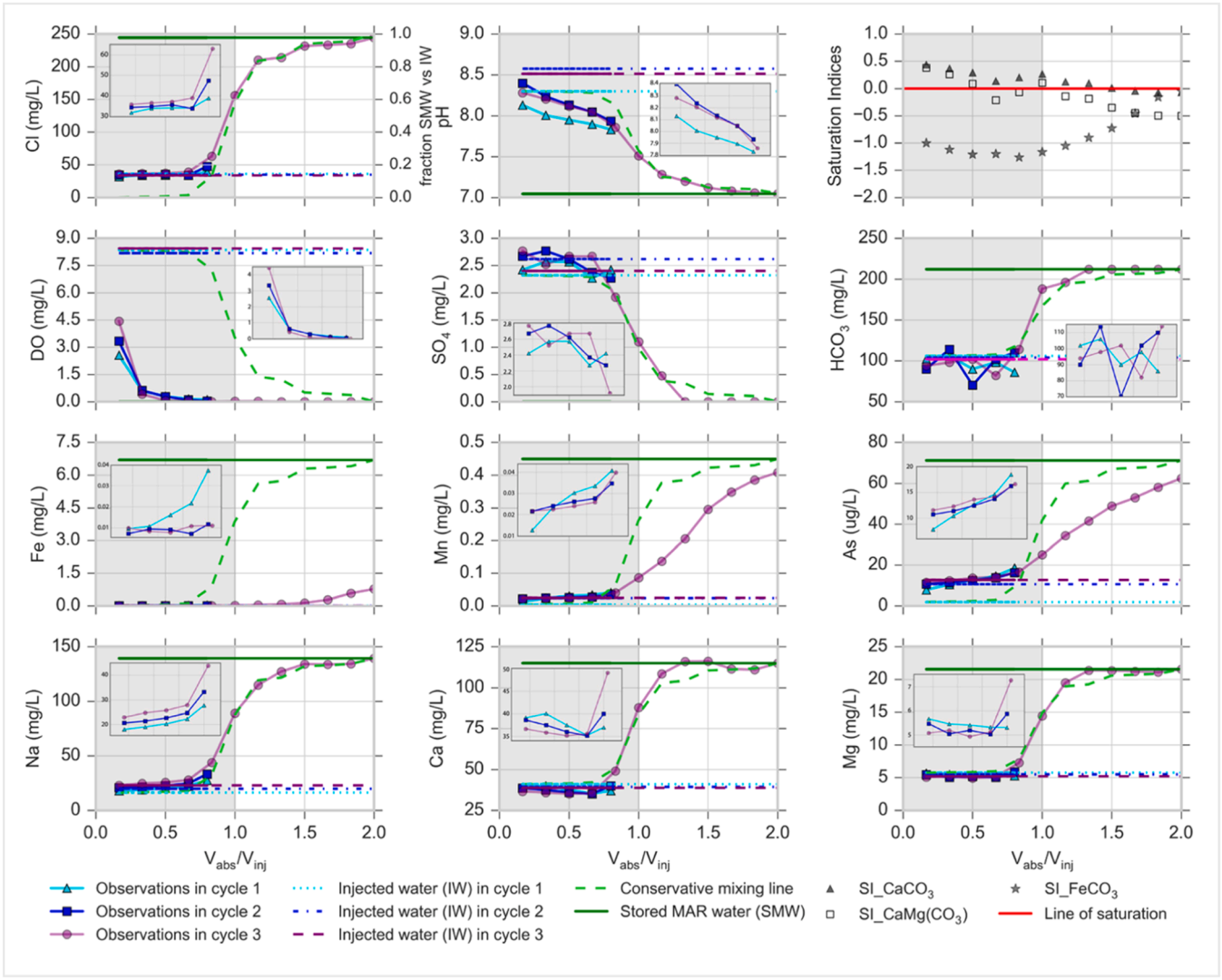

Fig. 4. Result of the oxidative (cyclic) push-pull test (PPT) at the abstraction well (OW 2) of site GMF11 (N 22° 37′ 18.05″, E 89° 50′ 9.72″) performed on 14/10/2018. Observations (cyan triangle, blue square, and purple dots as cycles 1,2 and 3, respectively), injected water composition (broken horizontal lines of cyan, blue, and purple as cycles 1,2 and 3, respectively), stored MAR water composition (horizontal green line), the calculated fraction of injected water based on Cl as conservative tracer measurements (lime green dashed line in Cl plot), and the calculated conservative concentrations of the various parameters based on conservative mixing calculations (lime green lines in rest of the panels) are shown against the abstracted divided by injected volume (V_{abs}/V_{inj}; V_{inj} = 300 L). In addition, the saturation indices of calcite, dolomite, and siderite are also shown in the last panel, plotted against the same axis. The solid red line indicates the line of saturation for the minerals shown in the plot. Enlarged insets for the initial observations are added to each panel to enhance the visibility of the slight changes during the successive cycles (V_{abs}/V_{inj}=0–0.8).

Table 4
Summary of measured onsite parameters in injected water during the push phase of oxidative PPTs as conducted at abstraction and/or monitoring wells at all sites based on the Figures S1-S4 and S8–11 in the supplement.

Parameters	GMF11 Abstr. Well.	GMF11 Mon. Well	JJS91 Abstr. Well.	JJS91 Mon. Well	MGS Abstr. Well.	MGS Mon. Well	MF05 (deep) Mon. Well	MF05 Mon. Well
EC	stable	stable	stable	stable	stable	stable		stable
Temp	increased by 0.7 °C in final cycle	stable	stable	stable	increased in 2nd & 3rd cycles	stable	stable	stable
pH	increased by 1.4 units in final cycle	stable	stable	stable	stable	stable	stable	stable
DO	fluctuates among cycles	fluctuates among cycles	fluctuates among cycles	fluctuates among cycles	decreased in 2nd & 3rd cycles	stable	fluctuates among cycles	decreased in cycles

indicate that the injected water composition remained constant throughout the injection.

Fig. 4 shows the sensed parameters, solute concentrations and saturation indices against the volume of abstracted water, normalized versus the volume of injection (i.e. V_{abs}/V_{inj}, where V_{inj}=300 L) during the oxidative (cyclic) PPT, which was performed at site GMF11 in the

abstraction well. Cl acted as a conservative tracer and showed dispersive mixing of injected water (cyan, blue, and purple broken lines for each cycle, respectively) with stored MAR water (solid green line). In addition, conservative mixing lines (based on cycle 1) were plotted as a dashed lime-green line in Fig. 4. To clarify: if only physical mixing processes would occur without any biogeochemical reactions during the PPT, then observed solute concentrations would be plotted on the conservative mixing line. Fig. 4 shows that at V_{abs}/V_{inj}= 1, the mixing fraction is 0.5, indicating the abstracted water is a 1:1 mixture of injected water and stored MAR water. The deviations between observed As, DO, Fe, or SO_4 concentrations and the conservative mixing line indicate the occurrence of hydrogeochemical reactions (Fig. 3A) affecting their concentrations.

The lower observed DO concentrations indicate a rapid consumption of DO in the aquifer compared to the conservative mixing line (Fig. 4). The DO level in the initial abstracted samples per cycle shows a rise due to the aeration before each injection cycle. Injected water became anoxic at $V_{abs}/V_{inj} = 0.8$. This rapid consumption of DO is most likely coupled to the oxidation of dissolved Fe, organic matter (OM), and/or pyrite (Antoniou et al., 2013; Kruisdijk and van Breukelen, 2021). Fig. 4 shows a slight rise in the concentration of SO_4 over the sequential cycles compared to the conservative mixing line: 1.5 ± 1.8 mg/L in cycle 1, 1.7 ± 2.4 mg/L in cycle 2, and 2.0 ± 3.4 mg/L in cycle 3. Antoniou et al. (2013); Kruisdijk and van Breukelen (2021); Zuurbier et al. (2016) found that the increased SO_4 concentrations may result from pyrite oxidation. During this oxidative PPT, not all O_2 is used for pyrite oxidation. This is because if all the O_2 were used, concentrations of SO_4 would have increased by about 13 mg/L based on the consumption of DO and pyrite oxidation stoichiometry as follows:

$$FeS_2 + \frac{7}{2}O_2 + H_2O \rightarrow \ Fe^{2+} + 2{SO_4}^{2-} + 2H^+ \quad (12)$$

$$4Fe^{2+} + O_2 + 10H_2O \rightarrow 4Fe(OH)_3 + 8H^+ \quad (13)$$

Despite the injection of low-As pond water (cycle 1 = 2 μg/L, cycle 2 = 10.5 μg/L, and cycle 3 = 12.7 μg/L), Fig. 4 shows an almost instant increase in As in cycle 1 (average of 12.8 μg/L), in cycle 2 and 3 (average of 12.9 μg/L) until $V_{abs}/V_{inj} = 0.7$, similar to that of SO_4. This almost instantaneous rise in As is attributed to the competitive desorption of As from Fe-(oxyhydr)oxides when low-As containing water was injected and the injected water replaced the stored MAR water with higher As concentrations (Rafiq et al., 2022). However, the slightly elevated concentrations of SO_4 and As compared to the mixing line at $V_{abs}/V_{inj} < 1$ indicate that As mobilization by the oxidation of arsenic-containing pyrite might also occur during this PPT. Table S2 in the supplement presents the geochemical characteristics of the sediment samples collected from two MAR sites: GMF11 and JJS91. Pyrite content in the sediment at this site was relatively low (0.04 % d.w.) compared to previously reported average values for the Bengal Delta basins (Nickson et al., 2000; Seddique et al., 2008). Relatively lower sedimentary pyrite content, the muted response of SO_4, and desorption of As due to the injection of low-As pond water suggest that pyrite oxidation does occur, but as a minor process in this aquifer, which is consistent with a previous study of Rafiq et al. (2022).

Another potential explanation for the consumption of DO is the oxidation of OM, which can be inferred from the increase in HCO_3 concentrations according to the following equations:

$$CH_2O + O_2 \rightarrow HCO_3^- + H^+ \quad (14)$$

A subtle increase (from 1.7 to 2.4 ± 4.1 mg/L in cycle 3) in the concentrations of HCO_3 was observed from $V_{abs}/V_{inj} = 1.5$ onwards. However, in case OM was the only reductant, a HCO_3 concentration increase of around 15 mg/L would have been expected based on the stoichiometry of OM oxidation in Eq. (14). Organic matter (OM) could be present in the aquifer as sedimentary OM (SOM) or, more likely, be introduced as dissolved organic carbon (DOC) during the injection of filtered pond water. During year-round monitoring at this site, the filtered pond and stored MAR water had an equal average DOC value of 9.5 mg/L, and native groundwater had a higher DOC level of 13.6 ± 1.2 mg/L (Rafiq et al., 2022). Because infiltration water is mixed with native groundwater (based on Cl values), a higher DOC would be expected compared to the measured value in stored water, which indicates the occurrence of DOC degradation (Rafiq et al., 2022). This suggests that the oxidation of SOM plays an insignificant role in DO consumption during oxidative PPT at this site. This could be different at other locations, as a relatively low SOM content (0.14 % d.w.) was observed at this site compared to the previously reported values for Holocene sediments in the Bengal delta basin (Anawar et al., 2010; McArthur et al., 2004; Nickson et al., 2000; Seddique et al., 2008).

The injection of fully aerated filtered pond water led to the oxidation of dissolved and (de)sorbed Fe, resulting in the formation of Fe-(oxyhydr)oxides. These newly formed Fe-(oxyhydr)oxides provide surface sites for sorption of dissolved Fe, Mn, and As. Consequently, decreased Fe, Mn, and As concentrations were observed compared to the conservative mixing line from V_{abs}/V_{inj}= 1.0 onwards (Fig. 4). This suggests the partial removal of Fe, Mn, and As by sorption onto newly formed Fe-(oxyhydr)oxides. Before conducting PPTs, Fe concentrations in the stored MAR water and native groundwater were 6.7 mg/L and 7.0 mg/L, respectively. When the MAR system was inactive at this site, the stored MAR water became depleted of O_2, resulting in anoxic conditions (Rafiq et al., 2022). Under these reducing conditions, Fe can be mobilized through the reductive dissolution of Fe-(oxyhydr)oxides. Furthermore, Fe can be released from aquifer sediments via cation exchange and surface complexation processes (Rahman et al., 2015; van Halem et al., 2009). Fig. 4 also shows a slight but noticeable decrease in pH values until $V_{abs}/V_{inj} = 1.0$ compared to the mixing line (pH decline ~ 0.5 pH units), which can be expected due to the oxidation of dissolved Fe in the aquifer during abstraction until $V_{abs}/V_{inj} = 1.0$ (Eq. (13)). However, the drop in pH levels could also be related to pyrite and OM oxidation (Eq. (12)–(14)). The observed partial removal of Fe, Mn, and As during this experiment closely resembles previously studied subsurface Fe and As removal techniques (SIR and SAR). These methods involve the periodic injection of O_2-rich water into an anoxic aquifer through tubewells. This process facilitates the oxidation of dissolved Fe, which consequently leads to the formation of Fe-(oxyhydr)oxides. These neoformed Fe-(oxyhydr)oxides then effectively sorb dissolved Fe and As on their surface, and low Fe and As water is abstracted from that well (Rahman et al., 2014, 2015; van Halem et al., 2010).

The injection of freshwater into the aquifer, which was filled with stored MAR water having a relatively higher salinity (EC = 0.26 versus 1.06 mS/cm, respectively), was expected to induce cation-exchange processes, reflecting the freshening of saline aquifers (Appelo and Postma, 2005). Fig. 4 shows a slight increase in Na (~0.21 meq/L) and a decrease in Ca (~0.24 meq/L) and Mg concentrations (~0.06 meq/L) compared to conservative mixing concentrations (grey portion, $V_{abs}/V_{inj} < 1$). For $V_{abs}/V_{inj} > 1$, an increase of Ca, Mg, and Na concentrations was observed compared to the mixing line, indicating no exchange between these cations. During abstraction, dissolved Fe was adsorbed on newly formed Fe-(oxyhydr)oxides. This might have resulted in the desorption of Ca and Na through cation exchange processes according to Eqs. (15) and (16). Note that it was difficult to comprehend any significant cation exchange processes during this PPT, as MAR operation before the PPT already resulted in fresher water compared to the native groundwater.

$$CaX \ + Fe^{2+} \rightarrow XFe \ + Ca^{2+} \quad (15)$$

$$2NaX \ + Fe^{2+} \leftrightarrow X_2Fe \ + 2Na^+ \quad (16)$$

At this site, DO was rapidly consumed upon injecting aerated filtered pond water into the aquifer filled with stored MAR water. Only subtle increases in SO_4 and alkalinity were observed, suggesting that pyrite and

sedimentary OM oxidation were insignificant. Instead, it is more likely that the majority of introduced O_2 was consumed by dissolved and (de) sorbed Fe. The adsorption of Fe^{2+} onto Fe-(oxyhydr)oxides caused a drop in pH (Appelo and Postma, 2005) and resulted in the removal of Fe (~99 %), Mn (~73 %), and As (~55 %) during the abstraction. However, when low-arsenic water was injected, As and some Mn were desorbed from the surface sites of Fe-(oxyhydr)oxides during the displacement of stored MAR water, initially resulting in elevated As levels in abstracted water.

3.3. Summary of the oxidative PPTs findings at JJS91, MGS and MF05 compared to GMF11

Besides at site GMF11, oxidative (cyclic) PPTs were also performed at sites JJS91, MF05, and MGS. In total, eight PPTs were conducted at four sites in the abstraction well and the monitoring well. The composition of injected water (EC, pH, DO, Temperature) during all PPTs was generally constant and only minor fluctuations were observed, as summarized in Table 4, based on the observations shown in Figures S2-S4; S8-S11. With successive cycles, the pH of injection water increased due to repeated aeration and CO_2 stripping (Appelo and Postma, 2005).

Table 5 summarizes the main results of the oxidative (cyclic) PPTs at all sites based on Fig. 4, Figures S5-S7 (PPTs conducted in abstraction wells), and Figures S12–15 (PPTs conducted in monitoring wells) in the supplement. The following section describes the key findings from this table for the other three sites compared to GMF11.

JJS91: The consumption of DO, decreased concentrations of Fe, Mn, and As, and cation exchange processes (Table 5 and Figure S5) were analogous to those observed at GMF11 (Fig. 4). However, SO_4 concentrations in the injected and stored MAR water were an order of magnitude higher than at GMF11 and consistently remained above the conservative mixing line throughout the third cycle (Figure S5). The initially elevated As (Figure S5) and concurrent SO_4 production suggest that pyrite oxidation may occur, in addition to desorption, thereby contributing to the initial mobilization of As. Hydrogeochemical processes observed during oxidative PPTs between the abstraction (Figure S5) and monitoring wells (Figure S13) were predominantly comparable, except for SO_4 and pH. Specifically, SO_4 concentrations in the abstraction well increased consistently throughout the PPTs (Figure S5), while in the monitoring well they decreased following an initial rise (Figure S13). Similarly, As concentrations in the abstraction well exhibited an early increase (Figure S5), whereas concentrations in the monitoring well remained below the conservative mixing line for most samples, apart from the first (Figure S13).

MGS: The consumption of DO and the reduction of Fe and Mn concentrations followed trends like those observed at sites GMF11 (Fig. 4) and JJS91 (Table 5 and Figure S6). The variation in SO_4 concentrations was observed differently depending on the well: in the abstraction well, they initially increased and subsequently decreased relative to the mixing line (Figure S6), whereas in the monitoring well, they continually decreased, suggesting that pyrite oxidation may occur but is not the predominant process (Figure S14). The injection of low-As water induced arsenic mobilization in both wells through desorption (Figure S6 and S14). Compared to the other two sites (Table 5), HCO_3 concentrations increased relative to the conservative mixing line throughout the pull phase (Figure S6). The concurrent increase in HCO_3 and pH indicates organic matter oxidation, with CO_2 production driving $CaCO_3$ dissolution and further elevating HCO_3 and pH (Figure S6). Overall, the hydrogeochemical processes during oxidative PPTs were consistent between the two wells (Figure S6 and S14), with only minor variations in SO_4 concentrations.

MF05: At site MF05, the abstraction well was non-functional, so a deep monitoring well was used to inject filtered pond water into the native groundwater instead of stored MAR water. Due to limited daylight, only two successive cycles were carried out. Unlike the other three sites (Table 5), decreased SO_4 and HCO_3 concentrations were observed compared to the conservative mixing line (Figure S7), indicating that oxidation of pyrite and organic matter was likely insignificant. Elevated As concentrations were observed relative to the mixing line (Figure S7), suggesting its mobilization; however, this can be attributed to the injected pond water, which contained higher As concentrations than the native groundwater. Overall, no significant differences in hydrogeochemical processes were observed between the oxidative PPTs conducted in the central deep monitoring well (Figure S7) and those in the other monitoring well (Figure S15).

3.4. Discussion on hydrogeochemical processes during oxidative PPTs at four MAR sites

Across all four sites, the DO was consumed rapidly upon the introduction of fully aerated filtered pond water. Most of the introduced DO was likely consumed by both dissolved and (de)sorbed Fe, resulting in the formation of fresh Fe-(oxyhydr)oxides. Consequently, the adsorption of dissolved Fe onto Fe-(oxyhydr)oxides significantly decreased Fe and Mn during abstraction across all sites and wells. Besides for Fe and Mn, decreased As levels were also observed at sites GMF11 and JJS91. The partial removal of these metals is consistent with subsurface Fe and As removal (SIR and SAR) techniques that rely on periodic injection of O_2-

Table 5
Overview of the main results of the oxidative PPTs at all sites based on Fig. 4, Figures S5-S7 (PPTs done in abstraction wells) and Figures S12–15 (PPTs done in monitoring wells) in the supplement. The change in water quality parameters (compared to conservative mixing) is expressed with an up-arrow (↑) and down-arrow (↓) for increasing and decreasing trends, while the size of the arrows signifies the magnitude of the change. A crossed marker (×) indicates the absence of any reactions. The division within certain cells suggests the changes in water quality parameters, where $V_{abs}/V_{inj} < 1$ is shown in the left cell and $V_{abs}/V_{inj} > 1$ in the right cell.

Parameters	GMF11 Abstr. Well.	GMF11 Mon. Well	JJS91 Abstr. Well	JJS91 Mon. Well	MGS Abstr. Well	MGS Mon. Well	MF05 (deep) Mon. Well	MF05 Mon. Well
pH	Slight decrease (↓) in pH until $V_{abs}/V_{inj} = 1$	↓ ↑	↑	↓ ↑	↑	↑	↓ ↑	↑
DO	Rapidly consumed and reached zero before $V_{abs}/V_{inj} = 1$, became anoxic in <2 hrs (↓)	↓	↓	↓	↓	↓	↓	↓
SO_4	slight rise over sequential cycles until V_{abs}/V_{inj} =0.7 (↑), then decreases (↓)	↑ ↓	↑	↑ ↓	↑	↑ ↓	↓	↓
As	a cyclic increase like that of SO_4 (↑), then decreased (↓)	↑ ↓	↑ ↓	↓	↑	↑	↑	↑
HCO_3	Subtle increase from $V_{abs}/V_{inj} = 1.5$, onwards (↑)	↓ ↑	↓	×	↑	↑ ↓	↓	↓
Fe & Mn	significantly decreased from $V_{abs}/V_{inj} = 1.0$, onwards (↓)	↓	↓	↓	↓	↓	↓	↓
Na, Ca & Mg	slight increase of Na (↑) and a decrease of Ca and Mg (↓) till $V_{abs}/V_{inj} = 1$	Na (↑/↓) Ca (↓/↑) Mg (↓)	Na (↑) Ca (↓/↑) Mg (↓/↑)	Na (↓) Ca (↓/↑) Mg (↓)	Na (↑) Ca (↑) Mg (↑)	Na (↓) Ca (↑) Mg (×)	Na (↑) Ca (↓) Mg (↓)	Na (↑) Ca (↓) Mg (↓)
SIs minerals	$CaCO_3$ precipitated (↓) and $FeCO_3$ dissolved (↑)	Ca/ $MgCO_3$(↓) $FeCO_3$(↑)	$CaCO_3$(↓) $FeCO_3$(↑)	Ca/ $MgCO_3$(↓) $FeCO_3$ (↑)	Ca/ $MgCO_3$(↓) $FeCO_3$(↑)	$CaCO_3$(↓) $FeCO_3$(↑)	Ca- $MgCO_3$(↓) $FeCO_3$ (↑)	Ca- $MgCO_3$(↓) $FeCO_3$ (↑)

rich water to precipitate Fe-(oxyhydr)oxides and sorb trace metals, like Fe, Mn, and As on their surfaces (Rahman et al., 2014, 2015; van Halem et al., 2010). Overall results of all sites confirm that Fe, Mn, and As concentrations decreased compared to the conservative mixing during the pull phases (from $V_{abs}/V_{inj} > 1.0$), indicating sorption and/or co-precipitation onto the newly formed Fe-(oxyhydr)oxides.

The initial rise in As concentrations during the pull phase (till $V_{abs}/V_{inj} < 1.0$) is mainly explained by desorption when low-As injected water displaced relatively higher-As stored MAR water at sites GMF11 and JJS91. In contrast, at site MGS, elevated As concentrations were observed throughout the pull phase for both the abstraction and the monitoring wells. At this site, the higher pH in the injected water results in desorption from Fe-(oxyhydr)oxide surfaces during the entire pull phase, thereby increasing the probability of As mobilization (Rafiq et al., 2022). Note that the As concentrations in the injected and stored MAR water were relatively low compared to those at other sites and remained below the WHO guideline value of 10 μg/L. At site MF05, elevated As concentrations were also observed, similar to those at MGS, during oxidative PPT in the deep and other monitoring wells. However, unlike the other sites, higher As levels in the injected water (As ~ 25–29 μg/L; Figures S7 and S15) were observed and the mobilization of As during the pull phase ($V_{abs}/V_{inj} > 1.0$) might also have occurred due to the desorption processes. At these two sites (MGS and MF05), sediment heterogeneity may have also influenced similar desorption processes, with varying injected water compositions. However, we did not collect any sediment samples from these two sites, and additional sediment samples are needed to demonstrate the geochemical heterogeneity between them.

Pyrite oxidation was minimal and varied depending on the aquifer condition across the four MAR sites. The initial slight increase in SO_4 concentrations at GMF11 and MGS and a more evident production of SO_4 at JJS91 suggest that some pyrite oxidation did occur during the oxidative PPTs. However, the low pyrite content at GMF11 and high background SO_4 concentrations at the other sites indicate that it was not the predominant process compared to oxidation of dissolved and (de) sorbed Fe. The oxidation of organic matter across the sites was generally limited. For example, a subtle increase in HCO_3 was observed at GMF11, which was much less than what we would expect if SOM were the main source of DO reduction. In contrast, a steady increase in bicarbonate concentrations and pH was observed at MGS, suggesting OM oxidation might have occurred, which was buffered by carbonate dissolution.

3.5. Rate constants for DO consumption during oxidative PPTs

Rapid DO consumption was observed during the oxidative PPTs at all four MAR sites. Fig. 5 presents the calculated first-order rate constants for DO consumption, with the associated errors per sequential cycle at the sites (A-D for GMF11, JJS91, MF05, and MGS) using the abstraction wells. These rate constants were derived from the slope of a best-fit line, where the logarithmic ratio of reactant concentrations (DO) to tracer concentrations (EC) was plotted against the residence time in the aquifer in minutes (Haggerty et al., 1998). Note that in this analysis, continuous DO sensor readings were used, obtained during the pull phases, as opposed to the DO levels measured in the grab samples collected during the PPTs.

The DO consumption curves did not originate from residence time = 0 at all PPT sites (Fig. 5) due to the time correction applied for the dead volume factor. This dead volume factor represents the minimum residence time when the injected water remains in the PPT well without reacting with the stored MAR water. Table 6 presents the determined first-order rate constants at each site and all cycles. The average first-order DO consumption rate constant ranges from ~53 day^{-1} at MGS to ~73 day^{-1} at JJS91. The first-order rate constant remained nearly stable with successive cycles, except at GMF11 and MGS. At site GMF11 (Fig. 5A), the DO rate constant increased by ~40 %, whereas at MGS (Fig. 5D), it somewhat decreased by ~5 % in the final cycle. Note that sites GMF11 and JJS91 (Fig. 5A and 5B) indicate a fast and consistent DO consumption rate with a good linear fit, whereas the model fit at sites MF05 and MGS (Fig. 5C and 5D) was poor. DO consumption kinetics was apparently more complex than the first-order model at those latter sites

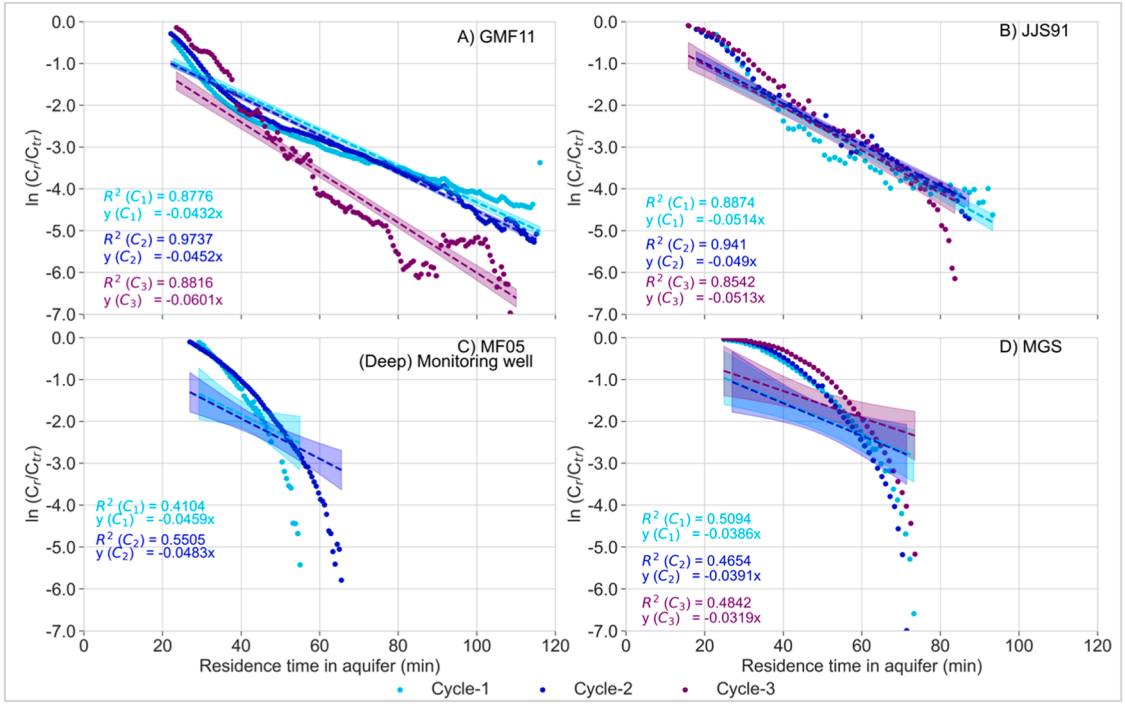

Fig. 5. The natural logarithm of the ratio of reactant concentrations (DO) to tracer concentrations (conductivity) is plotted against residence time in the aquifer (in minutes) at four MAR sites: (A) GMF11, (B) JJS91, (C) MF05, and (D) MGS using abstraction well, where the residence time is only considered until the DO levels in the abstracted samples reach zero. The best-fitted trendlines with a 95 % interval area are also drawn to determine the first-order rate constant, considering that these lines are constrained to (0,0).

Table 6
Comparison of the first-order DO consumption rate constants at the four (4) MAR sites.

Sites/Well	Cycles	k (min^{-1})	k (day^{-1})	R^2 values
GMF11	1	0.043	62.2	0.88
	2	0.045	65.1	0.97
	3	0.060	86.5	0.88
			71.3 (mean)	
JJS91	1	0.051	74.0	0.89
	2	0.049	70.6	0.94
	3	0.051	73.9	0.85
			72.8 (mean)	
MF05 (deep) Mon. Well	1	0.046	66.1	0.41
	2	0.048	69.6	0.55
			67.8 (mean)	
MGS	1	0.039	55.6	0.51
	2	0.039	56.3	0.47
	3	0.032	45.9	0.48
			52.6 (mean)	

(Fig. 5C and 5D). The DO data show initially none or slow consumption, and rapid consumption at later residence times and thus further away from the well into the aquifer. This suggests that the aquifer's reducing reactivity is high and constant at GMF11 and JJS91, whereas it is relatively low near the well and increases strongly away from the well, further into the aquifer at sites MF05 and MGS.

Table 7 compares the rate constants for DO consumption calculated with PPTs at our study sites with those reported in previous studies. Remarkably, the rate constants at our study sites are considerably higher than those reported in previous studies. The observed variation in the first-order rate constant for DO consumption is likely related to the geochemical properties of the aquifer and the availability and reactivity of reactants such as pyrite, organic matter, and dissolved or (de)sorbed Fe (Kruisdijk and van Breukelen, 2021). Given the subtle changes in SO_4 and alkalinity observed during oxidative PPTs (Sections 3.2 and 3.3), DO consumption by pyrite oxidation and organic matter is likely minimal. Instead, DO is consumed mostly through the oxidation of dissolved and (de)sorbed Fe, which proceeds through either homogeneous or heterogeneous oxidation mechanisms. Homogeneous Fe oxidation dominates when Fe is present primarily in the dissolved phase, and it proceeds at a very slow rate. In contrast, heterogeneous Fe oxidation occurs at the interface between the aqueous phase and solid surfaces, particularly in the presence of Fe-(oxyhydr)oxide minerals, and can be kinetically several orders of magnitude faster than homogeneous Fe oxidation. During the push phase of oxidative PPTs, the injected DO oxidized both dissolved and (de)sorbed Fe while displacing stored MAR water containing Fe^{2+}. This led to the formation of Fe-(oxyhydr)oxides and the generation of new sorption sites for available Fe^{2+} during abstraction. The presence of adsorbed Fe^{2+} on newly formed Fe-(oxyhydr)oxides rapidly accelerated DO consumption during the pull phase, as indicated by noticeably higher 1st order DO rate constants. This suggests that heterogeneous Fe oxidation is more likely to be the dominant process for DO consumption during oxidative PPTs at the researched MAR sites, which has been recognized as a key process in subsurface iron and arsenic removal technologies such as Subsurface Iron Removal (SIR) and Subsurface Arsenic Removal (SAR)(Rahman et al., 2014, 2015; van Halem et al., 2010).

Table 7
Literature overview of first-order rate constants for DO consumption (aerobic respiration) determined with PPTs.

	DO consumption rate constant (/day)	SOM (% d.w.)	Pyrite (% d.w.)	Aquifer materials
GMF11 (this study)	*71.3 (mean)*	*0.14*	*0.04*	*Very fine sand*
JJS91 (this study)	*72.8 (mean)*	*0.24*	*0.04*	*Very fine sand*
MGS (this study)	*52.6 (mean)*	-	-	-
MF05 (this study)	*67.8 (mean)*	-	-	-
Kruisdijk and van Breukelen (2021) 2021	2.5–3.8	0.4–1.0	0.05–0.53	Fine to coarse sands
Schroth et al. (1998)	3.6–40.0	-	-	Clayey silt and silt; petroleum contaminated
McGuire et al. (2002)	14.4	-	-	Sand contaminated with BTEX and chlorinated solvents
Vandenbohede et al. (2008)	8.8			Fine sand

3.6. Hydrogeochemical processes during reductive PPTs

Fig. 6 shows the results of the reductive PPTs performed at the same sites and wells as the oxidative PPTs. At sites GMF11 and JJS91, the abstraction and the monitoring well were used for reductive PPTs, whereas only the monitoring well was used at MGS and MF05. Sensor parameters and solute concentrations, including Cl, pH, Eh, DOC, HCO_3, acetate, Fe, Mn, As, Na, Ca, and SO_4 are shown against time since sucrose injection for all 6 PPTs in Fig. 6. The identical and stable concentrations of Cl and Na over time, as shown in Fig. 6, suggest that only the injected water was abstracted during the experiment, without significant dispersive mixing. The addition of sucrose to injection water leads to a sharp initial rise in DOC, followed by a gradual decrease over time at all PPT sites. HCO_3 concentrations increased by 2–3 times and gradually decreased over time (Fig. 6). Similarly, an initial rise in acetate concentrations was observed in Fig. 6, followed by a downward trend, except at GMF11 (abstraction well). Initially substantial decreases in pH and Eh were observed (Fig. 6). Furthermore, concentrations of Fe, Mn, and As increased considerably over time at all PPT sites, rising several-fold compared to the stored MAR water quality, followed by gradual to stronger declines over time. Fe concentrations increased the most (up to 590 times), followed by Mn (up to 40 times) and As (up to 3 times). The time required to reach peak concentrations for HCO_3, Fe, Mn, As, Ca, and Mg varied across sites, ranging from 30 to 60 h following sucrose injection. The concentrations of Fe, Mn, and As reached their highest levels approximately 40 h after sucrose injection, except for JJS91, where this occurred at ~25 and ~47 h in the abstraction and in the monitoring wells, respectively. Notably, As concentrations did not increase at sites MGS and MF05 (Fig. 6). A significant drop in pH and Eh occurred approximately 20 h after the sucrose injection. Fig. 6 also shows that the SO_4 concentrations decreased at all sites and wells during reductive PPTs, except at GMF11, where both the abstraction and the monitoring wells showed minimal change. The saturation indices (SIs) for calcite and dolomite in the abstracted water samples were below zero ($SI < 0$) at all sites, indicating undersaturation with respect to these minerals during reductive PPTs, except MGS, where the abstracted water samples were saturated. In contrast, SI for siderite was saturated to supersaturated at all sites except at MF05, where it was undersaturated to supersaturated.

The observed increase in HCO_3 and acetate concentrations can be attributed to the injection of sucrose-amended water following Eqs. (17)–(19). Sucrose, an easily degradable carbon source, decomposes into acetic acid (as acetate) and HCO_3 (Neidhardt et al., 2014; Rawson et al., 2017). Thus, the elevated concentrations of HCO_3 and acetate, and the drop in pH and DOC during the pull phase at all sites, suggest that sucrose degraded over time (eq. (17)–(19)). Additionally, acetate formation and its subsequent degradation resulted in a significant drop in pH values in the abstracted samples at all sites and wells (Fig. 6). The slightly acidic conditions during reductive PPTs likely induce the dissolution of calcite and/or dolomite, as indicated by saturation indices (SIs) below zero ($SI < 0$) for both minerals (Fig. 6), which explains the

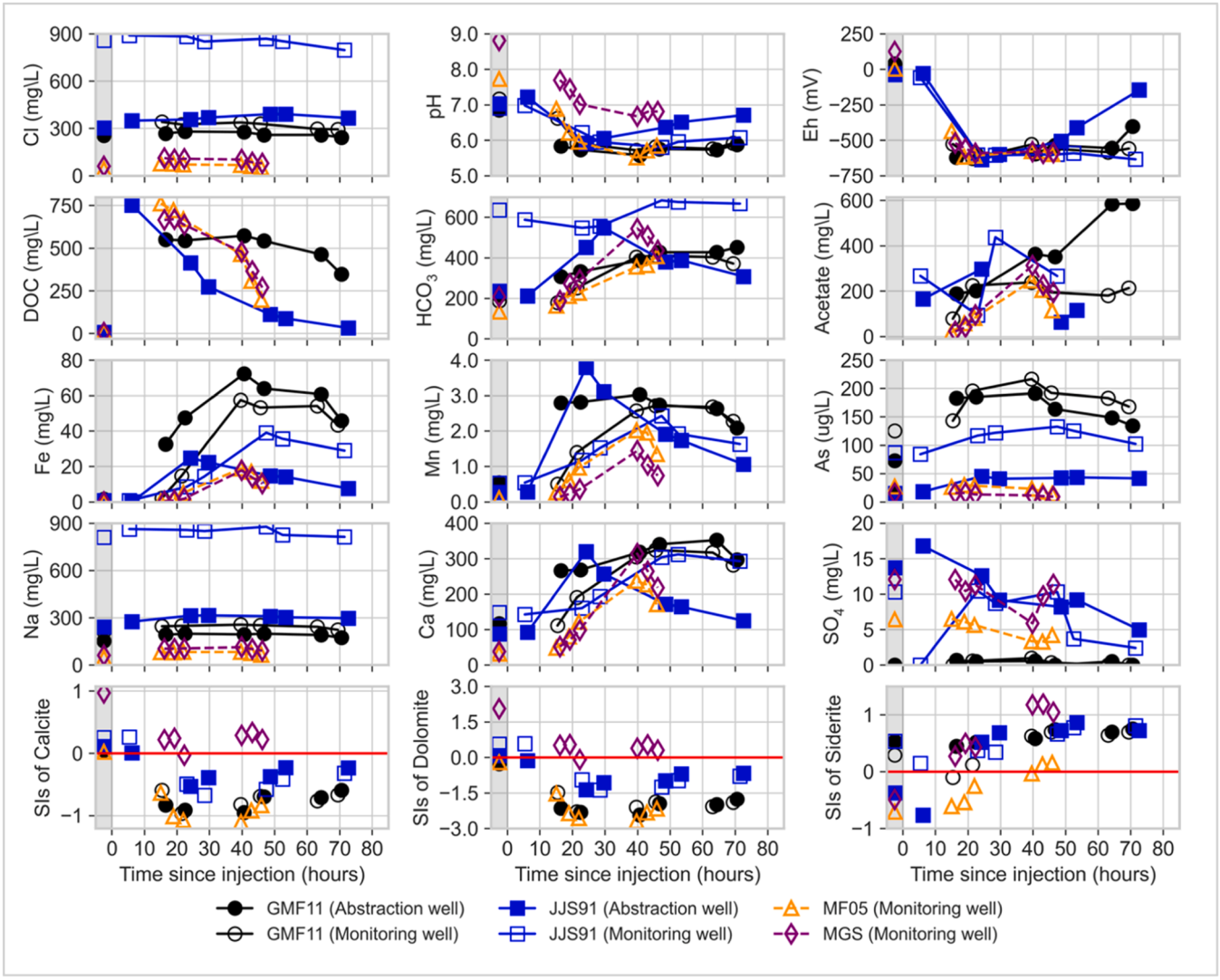

Fig. 6. Results of reductive PPTs performed during October-November 2018 at four MAR sites: GMF11, JJS91, MGS, and MF05. A different colour and marker represent each site. At sites GMF11 and JJS91, reductive PPTs were conducted using both abstraction (filled markers) and monitoring wells (unfilled markers), whereas only the monitoring wells were used at sites MF05 and MGS. In addition, the composition of the stored MAR water (SMW) prior to the PPTs is shown in the grey-coloured zone, where the same marker (without line) represents observations for each site. At each site, 300 L of stored MAR water was injected after adding sucrose and the same volume of the injected water was abstracted. The observed water quality parameters of abstracted water were plotted against time since the end of the push phase.

increased Ca concentrations during the pull phase.

$$C_{12}H_{22}O_{11} + H_2O \rightarrow 2C_6H_{12}O_6 \quad (17)$$

$$C_6H_{12}O_6 + 2H_2O \rightarrow 2CH_3COO^- + 2HCO_3^- + 2H^+ + 4H_2 \quad (18)$$

$$2CH_3COO^- + 8H_2O \rightarrow 4HCO_3^- + 18H^+ + 16e^- \quad (19)$$

The decomposition of sucrose into acetate, and the further degradation of acetate induced the reductive dissolution of Fe-(oxyhydr)oxides at PPT sites, leading to Fe, Mn, and As mobilization (Cai et al., 2021; Chapelle, 2000; Wu et al., 2018). The extremely low negative Eh values in Fig. 6 suggest that these metals were mobilized under strongly reduced conditions (Jurgens et al., 2009). Besides, the observed decline in SO_4 and substantial rise in Fe concentrations at most sites suggests the occurrence of microbial SO_4 reduction during reductive PPTs, except GMF11, where reductive dissolution of Fe-(oxyhydr)oxides seems the dominant process. However, despite a significant rise in Fe and Mn concentrations, As concentrations at sites MGS and MF05 did not increase substantially. The addition and degradation of sucrose leads to higher concentrations of Fe and HCO_3, promoting the formation of Fe-carbonate minerals such as siderite, which was previously observed in shallow groundwater of the Bengal Basin (Reza et al., 2013; Saha et al., 2020). The positive saturation indices (SIs) for siderite during the reductive PPTs support the potential for siderite precipitation at most sites. Arsenic could potentially been resorbed and/or coprecipitated on these newly formed Fe-carbonate minerals suggesting this minimal increase in As at sites MGS and MF05 (Neidhardt et al., 2014; Rawson et al., 2017). However, precipitation of FeS minerals due to the SO_4 reduction might have lower As levels through of co-precipitation. Additionally, the availability of Fe-associated As might have been limited at these sites (Neidhardt et al., 2014).

3.7. Insights from PPTs: how to improve MAR water quality?

During oxidative PPTs, O_2-saturated filtered pond water was injected into stored MAR water, resulting in rapid consumption of DO. The DO was primarily consumed by dissolved and (de)sorbed Fe, leading to the formation of Fe-(oxyhydr)oxides, while the oxidation of pyrite and

organic matter (OM) was insignificant to minor at all sites over successive cycles of oxidative PPTs. These Fe-(oxyhydr)oxides subsequently sorbed dissolved Fe, Mn, and As onto their surfaces, thereby immobilizing these elements in the abstracted water. The determined first-order rate constants for DO consumption were extremely high at all four MAR sites, and remained high with subsequent infiltration and abstraction cycles, indicating that heterogeneous Fe oxidation is likely the dominant mechanism driving DO consumption.

DO consumption through the oxidation of aquifer matrix materials has been widely observed in various aquifer recharge techniques worldwide. However, numerous studies have reported differing dominant reductants responsible for DO consumption, including pyrite, sedimentary organic matter (OM), and dissolved Fe(Antoniou et al., 2012; Fakhreddine et al., 2015, 2020; Wallis et al., 2010; Zuurbier et al., 2016, 2014). For instance, a recent study by Rafiq et al. (2022) observed that DO consumption during MAR was primarily coupled to the oxidation of dissolved and (de)sorbed Fe, with As mobilization resulting from its desorption from Fe (oxyhydr)oxides. However, Rafiq et al. (2022) did not quantify the DO consumption rate, which is addressed in the present work. In contrast, other studies have attributed DO consumption predominantly to pyrite oxidation, leading to As mobilization through the oxidative dissolution of As-bearing pyrite (Antoniou et al., 2013, 2012; Zuurbier et al., 2016, 2014). Similarly, recent work on PPTs in an aquifer storage and recovery (ASR) system in the Netherlands indicated that the reduction in O_2 and NO_3 concentrations was primarily driven by oxidation of sedimentary OM and pyrite (Kruisdijk and van Breukelen, 2021). Conversely, in this current study, the oxidation of OM and pyrite appeared to be minimal to insignificant compared to heterogeneous Fe oxidation. This difference may reflect the aquifer condition, where an anoxic, brackish aquifer has been recharged repeatedly with oxic source water. Consequently, reactive pyrite may already have been depleted, and the processes observed here may not entirely exemplify "fresh" MAR sites that have not experienced prior recharge but rather processes that can be expected in these MAR sites in the longer term.

In the reductive PPTs, a reactive carbon source (sucrose) was introduced into the stored MAR water, leading to increased concentrations of HCO_3 and acetate, and a decreased Eh and pH. These changes suggest that sucrose degraded over time, triggering excessive microbial reductive dissolution of Fe-(oxyhydr)oxides and mobilizing Fe, Mn, and As in the abstracted water. Therefore, the quality of the abstracted water deteriorated due to the elevated concentrations of these metals. Consistent with these findings, Neidhardt et al. (2014); Rawson et al. (2017) also observed the microbial reductive dissolution of Fe, Mn, and As due to the sucrose addition in the Bengal Delta Plain. Furthermore, numerous studies at MAR sites across South Asia support the claim that As mobilization frequently occurs due to the reductive dissolution of Fe-(oxyhydr)oxides under reduced conditions (Fakhreddine et al., 2021; Mailloux et al., 2013; Polizzotto et al., 2005).

The results of the reductive PPTs demonstrate the potential risk of Fe, Mn, and As mobilization due to intense microbial activity under reducing conditions. This poses a threat to drinking water safety, as the concentrations of these metals may exceed WHO guidelines. However, the reductive PPTs represent a worst-case scenario, with high concentrations of a highly reactive organic carbon source. In contrast, the study by Rafiq et al. (2022) indicates that the actual risk for Fe, Mn, and As mobilization is significantly lower during MAR operations, where the introduction of organic matter is limited both in terms of concentration and reactivity. This apparent inconsistency reflects disparities between short-term experimental perturbations (such as sucrose addition and rapid injection) and long-term infiltration processes (during MAR). Thus, while PPTs provide insight into mobilization mechanisms, the broader evidence indicates that MAR, as currently practiced at these sites, observed significantly lower As in stored MAR water compared to native groundwater and delivers a net positive impact to drinking water quality. To further lower this risk, it is recommended to ensure that concentrations of organic matter in injection water remain low. Further improvements to the sand filter, intended to remove suspended solids, may aid in this.

The findings of the oxidative PPTs suggest that oxic conditions favor the immobilization of Fe, Mn, and As, leading to improved water quality. The first-order rate constants for DO consumption show that infiltrated DO is rapidly consumed. Maintaining oxic conditions for the stored MAR water, therefore, appears challenging, particularly given the considerable distance (~3 m) between the infiltration wells and the abstraction well used for drinking water supply. To improve the quality of MAR water, it is recommended to maintain both infiltration and abstraction at high rates, such that the stored water bubble between infiltration and abstraction wells is replenished as frequently as possible, and the occurrence of anoxic conditions is prevented over time. In addition, flushing the water bubble in between infiltration and the central abstraction well several times with a strong oxidant like permanganate could be considered to completely oxidize this part of the aquifer in a limited amount of time (Antoniou et al., 2014).

4. Conclusions

This research was conducted on a total of 14 PPTs under oxidative and reductive conditions to study the hydrogeochemical processes affecting the (im)mobilization of Fe, Mn, and As at four (4) MAR sites in southwestern Bangladesh. The findings of the oxidative PPTs revealed extremely rapid consumption of dissolved oxygen (DO) with consecutive injection-abstraction cycles at all sites, suggesting that heterogeneous Fe oxidation is the key mechanism coupled to the rapid DO consumption. Despite slight increases and inconsistent changes in SO_4 and HCO_3 concentrations, the oxidation of pyrite and organic matter (OM) appeared to be insignificant to minor at all sites. Heterogeneous Fe oxidation, and subsequent formation of Fe-(oxyhydr)oxides, lead to the removal of Fe, Mn, and As through their sorption onto newly formed sorption sites. In contrast, the injection of low-As water led to the desorption of As from Fe-(oxyhydr)oxides at sites MGS and MF05. However, the As concentrations remained below the local drinking water standard of 50 μg/L at those sites. The reductive PPTs showed the degradation of the added sucrose in the stored MAR water. As a result, a sudden increase in alkalinity and acetate concentrations, accompanied by a drop in pH and Eh were observed in the abstracted water. This process induced the microbially mediated reductive dissolution of Fe-(oxyhydr)oxides, resulting in elevated Fe (~ 70 mg/L), Mn (~3.5 mg/L), and As (~120 μg/L) concentrations in the most extreme case, except at sites MGS and MF05, where the rise in As was minimal and likely due to co-precipitation of As on newly formed Fe-carbonate minerals. The key hydrogeochemical processes driving the mobilization of Fe, Mn, and As during the PPTs under oxidative and reductive conditions were similar between the PPTs conducted at the abstraction and the monitoring wells at the researched MAR sites, and differences were mostly observed among sites. The results indicate that MAR water quality can be improved through frequent flushing of the stored MAR water, which can be enhanced by the infiltration of O_2-rich water and increased abstraction. Furthermore, minimizing the input of organic matter in the infiltration water will aid in the prevention of reducing conditions which could trigger Fe, Mn, and As mobilization.

CRediT authorship contribution statement

Muhammad Risalat Rafiq: Writing – original draft, Writing – review & editing, Methodology, Investigation, Software, Visualization, Formal analysis, Data curation, Validation, Conceptualization. **Emiel Kruisdijk:** Writing – review & editing, Methodology, Validation, Software, Data curation. **Kazi Matin Ahmed:** Writing – review & editing, Supervision. **Louis C. Rietveld:** Writing – review & editing. **Boris M. van Breukelen:** Writing – review & editing, Methodology, Validation, Supervision, Project administration, Funding acquisition, Conceptualization.

Declaration of competing interest

The authors declare that they have no known competing financial interests or personal relationships that could have appeared to influence the work reported in this paper.

Acknowledgements

This work is part of the DeltaMAR project funded by the Urbanising Deltas of the World (UDW) programme of the Dutch Research Council NWO-WOTRO (Grant number: OND1357179). We gratefully acknowledge the support of Md. Saleh Shakeel Nomaan (University of Barishal) for assisting in the collection of water samples during the push-pull tests. We also thank Tasnim Alam Nafij (University of Barishal) for contributing illustrations to the graphical abstract and schematic layout of the MAR sites. We are grateful to Nadia van Pelt (Delft University of Technology) for her thorough proofreading and valuable suggestions on the flow and structure of the manuscript. Finally, we thank the three anonymous reviewers for their constructive comments, which substantially improved the quality of this paper.

Supplementary materials

Supplementary material associated with this article can be found, in the online version, at doi:10.1016/j.watres.2025.124878.

Data availability

Data will be made available on request.

References

Abedin, M.A., Collins, A.E., Habiba, U., and Shaw, R.J., 2019, Climate change, water scarcity, and health adaptation in Southwestern Coastal Bangladesh, vol. 10, no. 1, p. 28–42.

Ahmed, K.M., Bhattacharya, P., Hasan, M.A., Akhter, S.H., Alam, S.M.M., Bhuyian, M.A. H., Imam, M.B., Khan, A.A., Sracek, O., 2004. Arsenic enrichment in groundwater of the alluvial aquifers in Bangladesh: an overview. Applied Geochemistry 19 (2), 181–200.

Alam, M., Sultana, M., Nair, G.B., Sack, R.B., Sack, D.A., Siddique, A.K., Ali, A., Huq, A., Colwell, R.R., 2006. Toxigenic *ibrio cholerae* in the Aquatic Environment of Mathbaria, Bangladesh. Appl. Environ. Microbiol. 72 (4), 2849.

Anawar, H., Yoshioka, T., Konohira, E., Akai, J., Freitas, M., Tareq, S., 2010. Sources of organic carbon and depositional environment in the Bengal delta plain sediments during the Holocene period. Limnology. (Tokyo) 11, 133–142.

Annaduzzaman, M., Rietveld, L.C., Hoque, B.A., Bari, M.N., van Halem, D., 2020. Arsenic removal from iron-containing groundwater by delayed aeration in dual-media sand filters. J. Hazard. Mater., 124823

Antoniou, E.A., Hartog, N., van Breukelen, B.M., Stuyfzand, P.J., 2014. Aquifer pre-oxidation using permanganate to mitigate water quality deterioration during aquifer storage and recovery. Applied Geochemistry 50, 25–36.

Antoniou, E.A., Stuyfzand, P.J., van Breukelen, B.M., 2013. Reactive transport modeling of an aquifer storage and recovery (ASR) pilot to assess long-term water quality improvements and potential solutions. Applied Geochemistry 35, 173–186.

Antoniou, E.A., van Breukelen, B.M., Putters, B., Stuyfzand, P.J., 2012. Hydrogeochemical patterns, processes and mass transfers during aquifer storage and recovery (ASR) in an anoxic sandy aquifer. Applied Geochemistry 27 (12), 2435–2452.

Appelo, C.A.J., Postma, D., 2005. Geochemistry, Groundwater and Pollution. Balkema, Leiden.

Ayers, J.C., Goodbred, S., George, G., Fry, D., Benneyworth, L., Hornberger, G., Roy, K., Karim, M.R., Akter, F., 2016. Sources of salinity and arsenic in groundwater in southwest Bangladesh. Geochem. Trans. 17 (1), 4.

Aziz, Z., Bostick, B.C., Zheng, Y., Huq, M.R., Rahman, M.M., Ahmed, K.M., van Geen, A., 2017. Evidence of decoupling between arsenic and phosphate in shallow groundwater of Bangladesh and potential implications. Applied Geochemistry 77, 167–177.

Barker, J.L.B., Hassan, M.M., Sultana, S., Ahmed, K.M., Robinson, C.E., 2016. Numerical evaluation of community-scale aquifer storage, transfer and recovery technology: a case study from coastal Bangladesh. J Hydrol 540, 861–872.

Bhattacharya, P., Hasan, M.A., Sracek, O., Smith, E., Ahmed, K.M., von Brömssen, M., Huq, S.M.I., Naidu, R., 2009. Groundwater chemistry and arsenic mobilization in the Holocene flood plains in south-central Bangladesh. Environ. Geochem. Health 31 (1), 23–43.

Bhuiyan, M.A.H., Rakib, M.A., Dampare, S.B., Ganyaglo, S., Suzuki, S., 2011. Surface water quality assessment in the central part of Bangladesh using multivariate analysis. KSCE Journal of Civil Engineering 15 (6), 995–1003.

Biswas, A., Gustafsson, J.P., Neidhardt, H., Halder, D., Kundu, A.K., Chatterjee, D., Berner, Z., Bhattacharya, P., 2014. Role of competing ions in the mobilization of arsenic in groundwater of Bengal Basin: insight from surface complexation modeling. Water. Res. 55, 30–39.

Cai, X., ThomasArrigo, L.K., Fang, X., Bouchet, S., Cui, Y., Kretzschmar, R., 2021. Impact of organic matter on microbially-mediated reduction and mobilization of arsenic and iron in arsenic(V)-bearing ferrihydrite. Environ. Sci. Technol. 55 (2), 1319–1328.

Chakraborty, M., Mukherjee, A., Ahmed, K.M., 2015. A review of groundwater arsenic in the Bengal Basin, Bangladesh and India: from source to sink. Curr. Pollut. Rep. 1 (4), 220–247.

Chapelle, F.H., 2000, The significance of microbial processes in hydrogeology and geochemistry, vol. 8, no. 1, p. 41–46.

Das, D., Chatterjee, A., Samanta, G., Mandal, B., Roy Chowdhury, T., Pratim Chowdhury, P., Chanda, C., Basu, G., Lodh, D., 1995. Arsenic contamination in groundwater in 6 districts of West Bengal, India - the biggest arsenic calamity in the world. Analyst 119:N168-N170. Analyst 119, 168N–170N.

Fakhreddine, S., Dittmar, J., Phipps, D., Dadakis, J., Fendorf, S., 2015. Geochemical triggers of arsenic mobilization during managed aquifer recharge. Environ. Sci. Technol. 49 (13), 7802–7809.

Fakhreddine, S., Prommer, H., Gorelick, S.M., Dadakis, J., Fendorf, S., 2020. Controlling arsenic mobilization during managed aquifer recharge: the role of sediment heterogeneity. Environ. Sci. Technol. 54 (14), 8728–8738.

Fakhreddine, S., Prommer, H., Scanlon, B.R., Ying, S.C., Nicot, J.-P., 2021. Mobilization of arsenic and other naturally occurring contaminants during managed aquifer recharge: a critical review. Environ. Sci. Technol. 55 (4), 2208–2223.

Griffioen, J., Klein, J., van Gaans, P.F.M., 2012. Reaction capacity characterization of shallow sedimentary deposits in geologically different regions of the Netherlands. J. Contam. Hydrol. 127 (1), 30–46.

Haggerty, R., Schroth, M.H., and Istok, J.D., 1998, Simplified method of "push-pull" test data analysis for determining In situ reaction rate coefficients, vol. 36, no. 2, p. 314–324.

Harvey, C.F., Swartz, C.H., Badruzzaman, A.B.M., Keon-Blute, N., Yu, W., Ali, M.A., Jay, J., Beckie, R., Niedan, V., Brabander, D., Oates, P.M., Ashfaque, K.N., Islam, S., Hemond, H.F., Ahmed, M.F., 2002. Arsenic mobility and groundwater extraction in Bangladesh. Science (1979) 298 (5598), 1602.

Hasan, M.A., Ahmed, K.M., Sracek, O., Bhattacharya, P., von Brömssen, M., Broms, S., Fogelström, J., Mazumder, M.L., Jacks, G., 2007. Arsenic in shallow groundwater of Bangladesh: investigations from three different physiographic settings. Hydrogeol. J. 15 (8), 1507–1522.

Hasan, M.M., Ahmed, K.M., Sultana, S., Rahman, M.S., Ghosh, S.K., Ravenscroft, P., 2018. Investigations on groundwater buffering in Khulna-Satkhira Coastal Belt using managed aquifer recharge. In: Mukherjee, A. (Ed.), Groundwater of South Asia. Springer Singapore, Singapore, pp. 453–462.

Ho, L., Alonso, A., Eurie Forio, M.A., Vanclooster, M., Goethals, P.L.M., 2020. Water research in support of the Sustainable Development Goal 6: a case study in Belgium. J. Clean. Prod. 277, 124082.

Horneman, A., van Geen, A., Kent, D.V., Mathe, P.E., Zheng, Y., Dhar, R.K., O'Connell, S., Hoque, M.A., Aziz, Z., Shamsudduha, M., Seddique, A.A., Ahmed, K.M., 2004. Decoupling of As and Fe release to Bangladesh groundwater under reducing conditions. Part I: evidence from sediment profiles1 1Associate editor: G. Sposito. Geochim. Cosmochim. Acta 68 (17), 3459–3473.

Istok, J.D., 2012. Push-pull Tests For Site Characterization. Springer Science & Business Media.

Istok, J.D., Humphrey, M.D., Schroth, M.H., Hyman, M.R., and O'Reilly, K.T., 1997, Single-well, "push-pull" test for In situ determination of microbial activities, vol. 35, no. 4, p. 619–631.

Jurgens, B., McMahon, P., and Chapelle, F., 2009, An Excel® workbook for identifying redox processes in ground water.

Khan, A.E., Scheelbeek, P.F.D., Shilpi, A.B., Chan, Q., Mojumder, S.K., Rahman, A., Haines, A., Vineis, P., 2014. Salinity in drinking water and the risk of (Pre)eclampsia and gestational hypertension in coastal Bangladesh: a case-control study. PLoS. One 9 (9), e108715.

Kim, Y., H Kim, J., H Son, B., Oa, S.-W., 2005. A single well push-pull test method for in situ determination of denitrification rates in a nitrate-contaminated groundwater aquifer: water science and technology. a journal of the International Association on Water Pollution Research 52, 77–86.

Kruisdijk, E., Eisfeld, C., Stuyfzand, P.J., van Breukelen, B.M., 2022. Denitrification kinetics during aquifer storage and recovery of drainage water from agricultural land. Science of The Total Environment 849, 157791.

Kruisdijk, E., van Breukelen, B.M., 2021. Reactive transport modelling of push-pull tests: a versatile approach to quantify aquifer reactivity. Applied Geochemistry 131, 104998.

Küfeoğlu, S., 2022. SDG-6 Clean Water and Sanitation, Emerging Technologies: Value Creation For Sustainable Development. Springer International Publishing, Cham, pp. 289–304.

Lowers, H.A., Breit, G.N., Foster, A.L., Whitney, J., Yount, J., Uddin, M.N., Muneem, A. A., 2007. Arsenic incorporation into authigenic pyrite, Bengal Basin sediment, Bangladesh. Geochim. Cosmochim. Acta 71 (11), 2699–2717.

Mailloux, B.J., Trembath-Reichert, E., Cheung, J., Watson, M., Stute, M., Freyer, G.A., Ferguson, A.S., Ahmed, K.M., Alam, M.J., Buchholz, B.A., Thomas, J., Layton, A.C., Zheng, Y., Bostick, B.C., Geen, A.v., 2013. Advection of surface-derived organic carbon fuels microbial reduction in Bangladesh groundwater. Proceedings of the National Academy of Sciences 110 (14), 5331–5335.

McArthur, J.M., Banerjee, D.M., Hudson-Edwards, K.A., Mishra, R., Purohit, R., Ravenscroft, P., Cronin, A., Howarth, R.J., Chatterjee, A., Talukder, T., Lowry, D., Houghton, S., Chadha, D.K., 2004. Natural organic matter in sedimentary basins and its relation to arsenic in anoxic ground water: the example of West Bengal and its worldwide implications. Applied Geochemistry 19 (8), 1255–1293.

McArthur, J.M., Ravenscroft, P., Safiulla, S., Thirlwall, M.F., 2001. Arsenic in groundwater. Testing pollution mechanisms for sedimentary aquifers in Bangladesh 37 (1), 109–117.

McGuire, J.T., Long, D.T., Klug, M.J., Haack, S.K., Hyndman, D.W., 2002. Evaluating Behavior of Oxygen, Nitrate, and Sulfate during Recharge and Quantifying Reduction Rates in a Contaminated Aquifer. Environmental Science & Technology 36, 2693–2700.

Missimer, T., Maliva, R., 2010. Aquifer storage and recovery and managed Aquifer recharge using wells. Planning, Hydrogeology, Design, and Operation.

Mladenov, N., Zheng, Y., Miller, M.P., Nemergut, D.R., Legg, T., Simone, B., Hageman, C., Rahman, M.M., Ahmed, K.M., McKnight, D.M., 2010. Dissolved organic matter sources and consequences for iron and arsenic mobilization in Bangladesh aquifers. Environ. Sci. Technol. 44 (1), 123–128.

Naus, F.L., Schot, P., Groen, K., Ahmed, K.M., Griffioen, J., 2019. Groundwater salinity variation in Upazila Assasuni (southwestern Bangladesh), as steered by surface clay layer thickness, relative elevation and present-day land use. Hydrol. Earth. Syst. Sci. 23 (3), 1431–1451.

Naus, F.L., Schot, P., van Breukelen, B.M., Ahmed, K.M., Griffioen, J., 2021. Potential for managed aquifer recharge in southwestern Bangladesh based on social necessity and technical suitability. Hydrogeol. J. 29 (2), 607–628.

Neidhardt, H., Berner, Z.A., Freikowski, D., Biswas, A., Majumder, S., Winter, J., Gallert, C., Chatterjee, D., Norra, S., 2014. Organic carbon induced mobilization of iron and manganese in a West Bengal aquifer and the muted response of groundwater arsenic concentrations. Chem. Geol. 367, 51–62.

Neil, C.W., Yang, Y.J., Jun, Y.-S., 2012. Arsenic mobilization and attenuation by mineral–water interactions: implications for managed aquifer recharge. Journal of Environmental Monitoring 14 (7), 1772–1788.

Nickson, R.T., McArthur, J.M., Ravenscroft, P., Burgess, W.G., Ahmed, K.M., 2000. Mechanism of arsenic release to groundwater, Bangladesh and West Bengal. Applied Geochemistry 15 (4), 403–413.

Parkhurst, D.L., Appelo, C., 1999. User's guide to PHREEQC (Version 2): a computer program for speciation, batch-reaction, one-dimensional transport, and inverse geochemical calculations. Water-resources investigations report 99 (4259), 312.

Polizzotto, M.L., Harvey, C.F., Sutton, S.R., Fendorf, S., 2005. Processes conducive to the release and transport of arsenic into aquifers of Bangladesh. Proceedings of the National Academy of Sciences 102 (52), 18819–18823.

Pyne, R.D., 2017. Groundwater Recharge and wells: a Guide to Aquifer Storage Recovery. Routledge.

Radloff, K.A., Zheng, Y., Stute, M., Weinman, B., Bostick, B., Mihajlov, I., Bounds, M., Rahman, M.M., Huq, M.R., Ahmed, K.M., Schlosser, P., van Geen, A., 2017. Reversible adsorption and flushing of arsenic in a shallow, holocene aquifer of Bangladesh: applied geochemistry. journal of the International Association of Geochemistry and Cosmochemistry 77, 142–157.

Rafiq, M.R., Ahmed, K.M., Rietveld, L.C., van Breukelen, B.M., 2022. Monitoring and inverse modelling of hydrogeochemical processes during managed aquifer recharge in Southwestern Bangladesh. Applied Geochemistry, 105472.

Rahman, M., Bakker, M., Borges Freitas, S., Halem, D., van Breukelen, B., Ahmed, K.M., and Badruzzaman, A., 2014, Exploratory experiments to determine the effect of alternative operations on the efficiency of subsurface arsenic removal in rural Bangladesh.

Rahman, M.M., Bakker, M., Patty, C.H.L., Hassan, Z., Röling, W.F.M., Ahmed, K.M., van Breukelen, B.M., 2015. Reactive transport modeling of subsurface arsenic removal systems in rural Bangladesh. Science of The Total Environment 537, 277–293.

Ravenscroft, P., Burgess, W.G., Ahmed, K.M., Burren, M., Perrin, J.J.H.J., 2005. Arsenic in groundwater of the Bengal Basin, Bangladesh. Distribution, field relations, and hydrogeological setting 13 (5), 727–751.

Rawson, J., Siade, A., Sun, J., Neidhardt, H., Berg, M., Prommer, H., 2017. Quantifying reactive transport processes governing arsenic mobility after injection of reactive organic carbon into a Bengal Delta aquifer. Environ. Sci. Technol. 51 (15), 8471–8480.

Reza, A.H.M.S., Jean, J.-S., Bundschuh, J., Liu, C.-C., Yang, H.-J., Lee, C.-Y., 2013. Vertical geochemical variations and arsenic mobilization in the shallow alluvial aquifers of the Chapai-Nawabganj District, northwestern Bangladesh: implication of siderite precipitation. Environ. Earth. Sci. 68 (5), 1255–1270.

Saha, N., Bodrud-Doza, M., Islam, A.R.M.T., Begum, B.A., Rahman, M.S., 2020. Hydrogeochemical evolution of shallow and deeper aquifers in central Bangladesh: arsenic mobilization process and health risk implications from the potable use of groundwater. Environ. Earth. Sci. 79 (20), 477.

Sarker, M.M.R., Van Camp, M., Hermans, T., Hossain, D., Islam, M., Uddin, M.Z., Ahmed, N., Bhuiyan, M.A.Q., Karim, M.M., Walraevens, K., 2021. Geophysical delineation of freshwater–Saline water interfaces in coastal area of Southwest Bangladesh. Water. (Basel) 13 (18), 2527.

Sarker, M.M.R., Van Camp, M., Islam, M., Ahmed, N., Walraevens, K., 2018. Hydrochemistry in coastal aquifer of southwest Bangladesh: origin of salinity. Environ. Earth. Sci. 77 (2), 39.

Savage, K.S., Tingle, T.N., O'Day, P.A., Waychunas, G.A., Bird, D.K., 2000. Arsenic speciation in pyrite and secondary weathering phases, Mother Lode Gold District, Tuolumne County, California. Applied Geochemistry 15 (8), 1219–1244.

Schroth, M.H., and Istok, J.D., 2006, Models to determine first-order rate coefficients from single-well push-pull tests, vol. 44, no. 2, p. 275–283.

Schroth, M.H., Istok, J.D., Conner, G.T., Hyman, M.R., Haggerty, R., O'Reilly, K.T., 1998. Spatial Variability in In Situ Aerobic Respiration and Denitrification Rates in a Petroleum-Contaminated. Aquifer 36, 924–937.

Schroth, M.H., Kleikemper, J., Bolliger, C., Bernasconi, S.M., Zeyer, J., 2001. In situ assessment of microbial sulfate reduction in a petroleum-contaminated aquifer using push-pull test and stable sulfur isotope analyses. J. Contam. Hydrol. 51, 179–195.

Seddique, A.A., Masuda, H., Mitamura, M., Shinoda, K., Yamanaka, T., Itai, T., Maruoka, T., Uesugi, K., Ahmed, K.M., Biswas, D.K., 2008. Arsenic release from biotite into a holocene groundwater aquifer in Bangladesh. Applied Geochemistry 23 (8), 2236–2248.

Sultana, S., Ahmed, K.M., Mahtab-Ul-Alam, S.M., Hasan, M., Tuinhof, A., Ghosh, S.K., Rahman, M.S., Ravenscroft, P., Zheng, Y., 2015. Low-cost aquifer storage and recovery. Implications for Improving Drinking Water Access for Rural Communities in Coastal Bangladesh 20 (3), B5014007.

van Breukelen, B., Röling, W., Groen, J., Griffioen, J., and W van Verseveld, H., 2003, Biogeochemistry and isotope geochemistry of a landfill leachate plume, 245–268 p:.

van Halem, D., Bakker, S.A., Amy, G.L., van Dijk, J.C., 2009. Arsenic in drinking water: a worldwide water quality concern for water supply companies: drink. Water Eng. Sci. 2 (1), 29–34.

van Halem, D., Heijman, S.G.J., Johnston, R., Huq, I.M., Ghosh, S.K., Verberk, J.Q.J.C., Amy, G.L., van Dijk, J.C., 2010. Subsurface iron and arsenic removal: low-cost technology for community-based water supply in Bangladesh. Water Science and Technology 62 (11), 2702–2709.

Vandenbohede, A., Louwyck, A., Lebbe, L., 2008. Identification and reliability of microbial aerobic respiration and denitrification kinetics using a single-well push–pull field test. J. Contam. Hydrol. 95 (1), 42–56.

von Brömssen, M., Häller Larsson, S., Bhattacharya, P., Hasan, M.A., Ahmed, K.M., Jakariya, M., Sikder, M.A., Sracek, O., Bivén, A., Doušová, B., Patriarca, C., Thunvik, R., Jacks, G., 2008. Geochemical characterisation of shallow aquifer sediments of Matlab Upazila, southeastern Bangladesh — Implications for targeting low-As aquifers. J. Contam. Hydrol. 99 (1), 137–149.

Wallis, I., Prommer, H., Simmons, C.T., Post, V., Stuyfzand, P.J., 2010. Evaluation of conceptual and numerical models for arsenic mobilization and attenuation during managed aquifer recharge. Environ. Sci. Technol. 44 (13), 5035–5041.

Wu, S., Fang, G., Wang, D., Jaisi, D.P., Cui, P., Wang, R., Wang, Y., Wang, L., Sherman, D. M., Zhou, D., 2018. Fate of As(III) and As(V) during microbial reduction of arsenic-bearing ferrihydrite facilitated by activated carbon. ACS Earth and Space Chem. 2 (9), 878–887.

Zheng, Y., Stute, M., van Geen, A., Gavrieli, I., Dhar, R., Simpson, H.J., Schlosser, P., Ahmed, K.M., 2004. Redox control of arsenic mobilization in Bangladesh groundwater. Appl. Geochem. 19 (2), 201–214.

Zuurbier, K.G., Hartog, N., Stuyfzand, P.J., 2016. Reactive transport impacts on recovered freshwater quality during multiple partially penetrating wells (MPPW-) ASR in a brackish heterogeneous aquifer. Appl. Geochem. 71, 35–47.

Zuurbier, K.G., Zaadnoordijk, W.J., Stuyfzand, P.J., 2014. How multiple partially penetrating wells improve the freshwater recovery of coastal aquifer storage and recovery (ASR) systems: a field and modeling study. J Hydrol 509, 430–441.